Aleksandra Inês Mazurek Vieira de Azevedo
Bachelor Degree in Biotechnological Engineering

Molecular studies on HSV: replication rate, infection capacity and progeny

Dissertation to obtain the Master of Science Degree in Molecular Genetics and Biomedicine

Supervisor: Sílvia Maria Milheiro Lopo Esteves, PhD,
Instituto Nacional de Saúde Doutor Ricardo Jorge
Co-Supervisor: Alexandra Isabel Cardoso Nunes, PhD,
Instituto Nacional de Saúde Doutor Ricardo Jorge

Jury:

President: Prof. Doutora Ilda Maria Barros dos Santos Gomes Sanches
Arguer: Prof. Doutora Filomena Ribeiro Alcobia da Silva Trabucho Caeiro
Member: Doutora Sílvia Maria Milheiro Lopo Esteves

FACULDADE DE CIÊNCIAS E TECNOLOGIA
UNIVERSIDADE NOVA DE LISBOA

Lisbon, 2016

NOVA University of Lisbon

Faculty of Sciences and Technology

Department of Life Sciences

Aleksandra Inês Mazurek Vieira de Azevedo

Molecular studies on HSV: replication rate, infection capacity and progeny

Dissertation to obtain a Master of Science Degree
in Molecular Genetics and Biomedicine,
from the NOVA University of Lisbon,
Faculty of Sciences and Technology

Supervisor:
Sílvia Maria Milheiro Lopo Esteves, PhD,
Instituto Nacional de Saúde Doutor Ricardo Jorge.
Co-Supervisor:
Alexandra Isabel Cardoso Nunes, PhD,
Instituto Nacional de Saúde Doutor Ricardo Jorge.

Lisbon, 2016

Molecular studies on HSV: replication rate, infection capacity and progeny

Notes of the author

The work described in this MSc thesis was carried out at the National Reference Laboratory of Herpes Simplex Virus, Citomegalovirus and Parvovirus B19 of the Infectious Diseases Department from the National Institute of Health, Lisbon, Portugal.

Acknowledgments

First, I would like to thank Dr. Fernando de Almeida, president of the National Institute of Health INSA and Dr. Jorge Machado, head of the department of infectious diseases, for allowing me to develop my theses in the institute and for the opportunity given to work in its laboratories.

I would like to express my special appreciation and gratitude to my supervisor, Dr. Silvia Lopo for always keeping an open door for me, for advising me, for helping with my many questions. Thank you for the support and encouragement words, and especially for your patience. I can assure you that without your help, I wouldn't have able to finish this work with a sane mind!

To my co-supervisors, Dr. Alexandra Nunes and Dr. João Paulo, for always pushing me to be better and aim higher. Thank you for the help, for stimulating interesting discussions and for teaching me the ways of this new world.

To Dr. Maria José, Carla, Ana Rita, Rita, Marta and Vitor from INSA for the help and the patience, for the lunches and the talks, for the jokes and the cheerful times. To Miguel, for the much needed help, and for the perseverance when I had almost lost hope!

To Professor Jaime Mota, from FCT, for helping me with one of the most important parts of this experimental work, and without whom it wouldn't have been done.

I would like to specially thank my family. Words cannot express how grateful I am for having you in my life, whether you're far or near. First, to my parents, for always supporting me in the decisions I made, and for advising me when stress got in the way; for believing in me, for saying that everything would eventually work out and for listening to me in my most frustrated moments. I know life hasn't been fair to us, but we somehow manage to overcome it!

To my sister Kika for always keeping a sane and clear mind towards me, and for annoying me in that singular way that only she knows (!); for the late McDonalds meals and ice-creams to overcome the worst days. Your endless source of support was vital to finish this work!

To my Portuguese grandmother, for always listening to me, and for distracting me in the most stressful times, even though it wasn't always easy for her.

To my polish grandparents, aunt and cousin, for the cheering, the support and the encouragement words. Maybe one day I'll get a job in Poland and we'll see each other more often!!

To my friends, for always being there, never complaining about hearing me babbling about my numerous problems, for the dinners and the lunches, for the dancing and the cheering.

Thank you! Obrigado! Dziękuję!

Resumo

Os vírus herpes simplex (HSV) são vírus ubíquos, adaptados ao hospedeiro, e responsáveis por diversas patologias. Existem dois subtipos: HSV-1, tradicionalmente associado a infeções a nível orofacial, e HSV-2, o qual é maioritariamente associado a úlceras genitais. Esta distinção é cada vez menos evidente, dada a emergência de infeções genitais causadas pelo HSV-1, associada sobretudo a fatores sociais, demográficos e migratórios, o que torna o herpes genital uma das infeções sexualmente transmissíveis mais prevalentes mundialmente.

Uma melhor compreensão das infeções genitais causadas pelo HSV-1 e HSV-2 é mandatória para entender a patogenicidade das doenças herpéticas. Esta tese teve como objetivo avaliar o ciclo de vida de vários isolados clínicos genitais de HSV-1 e HSV-2 com diferentes cargas virais, em linhas celulares distintas, dando ênfase à capacidade e eficiência da infeção viral, em termos de taxa de replicação e progenia.

Os nossos resultados mostraram que: i) ambos os subtipos do HSV apresentam um padrão de infeção semelhante independentemente da MOI, com DNA a ser sintetizado 6-12h pós-infeção; ii) independentemente do subtipo, a concentração inicial do vírus aparentemente não afeta a sua capacidade de adesão a qualquer linha celular; iii) as células Vero E6 mostraram-se as mais apropriadas para a infeção do HSV-2; iv) as células HeLa229 mostraram ser as mais apropriadas para a infeção do HSV-1 com cargas virais menores; e v) as células Vero apresentaram os piores resultados de infeção viral para ambos os subtipos. Em geral, o HSV-2 mostrou sempre menores capacidades de aderência e taxas de crescimento que o observado para o HSV-1, apesar de se terem observado maiores progenias na linha celular Vero E6.

Em conclusão, os resultados apresentados nesta tese de mestrado irão certamente contribuir para um melhor conhecimento da patogenicidade das infeções genitais causadas pelo herpes.

Palavras-chave: HSV-1, HSV-2, Herpes genital, Capacidade de infeção, Progenia, Cultura celular

Abstract

Herpes simplex viruses (HSV) are ubiquitous host-adapted pathogens that cause a variety of different disorders. There are two sub-types: HSV-1, which is traditionally associated with oro-facial infections, and HSV-2 that is mostly associated with genital ulcers. This distinction, however, is becoming less evident since HSV-1 frequency in genital infections is increasing due to social, demographic and migratory tendencies, making genital herpes one of the most prevalent sexually transmitted infections worldwide.

A better understanding on genital HSV-1 and HSV-2 infections is mandatory to the pathogenesis of human herpes disease. The scope of this thesis was to evaluate the life cycle of various HSV-1 and HSV-2 genital clinical isolates with different viral loads in three distinct host cell lines, giving special focus on both capacity and efficiency of viral infection, in terms of replication rate and progeny.

Our results showed that: *i*) both HSV-1 and HSV-2 isolates exhibited similar infection patterns regardless MOI, with DNA starting to be synthesized nearly at 6-12h post-infection; *ii*) regardless HSV subtype, initial viral concentrations do not apparently affect adherence to any host cell line nor the generated progeny; *iii*) Vero E6 cells seemed the most appropriated cell line for HSV-2 infection; *iv*) HeLa229 cells appeared to be the most suitable for HSV-1 infection for smaller inoculums; and *v*) Vero cell line had the worst viral growth results for both HSV subtypes. In general, HSV-2 displayed always lower both attachment capacities and growth rates than HSV-1, although higher progenies were seen in Vero E6 cell line.

Overall, the findings presented in this MSc thesis will certainly constitute a step forward for the understanding of the pathogenesis of the human herpes genital infections.

Key words: HSV-1, HSV-2, Genital Herpes, Infection capacity, Progeny, Cell culture

Thesis Outline

This MSc thesis is divided into 4 chapters that encompass:

i) a general introduction (Chapter 1) that intends to briefly describe the biology of Herpes Simplex Virus (HSV), in particular the current knowledge on HSV infections, clinical outcomes and infectious life cycle. The issues focused on this chapter aim to put into context and to emphasize the relevance of the study described throughout the thesis. Ultimately, the detailed aims of the present MSc thesis are presented;

ii) a section of materials and methods (Chapter 2) describing, in detail, the methodology used in the present thesis, including preliminary assays done for optimizing the experimental conditions for the current study;

iii) a results section (Chapter 3), where the main findings of the current study are presented, in order to better understand whether the HSV host cell invasion process depends on the genital HSV sub-type/strain or on the infected cell line, in terms of capacities of infections, replication rates, and progenies.

iv) an overall discussion and final conclusions (Chapter 4) where the major findings of the performed study are highlighted and discussed in a general context, taking into account the scope of this thesis.

The study presented on this thesis resulted on the following scientific communication:

A. Azevedo, A. Nunes, C. Roque, I. Costa, JP Gomes, S. Lopo. 2016. Molecular studies on HSV: replication rate, infection capacity and progeny. 19th Annual European Society for Clinical Virology Meeting, Lisbon, Portugal, 14-17 September 2016.

Table of contents

Figure index

Table index

Abbreviation List

3-OS-HS - 3-O sulfated heparan sulfate
ATCC - American Type Culture Collection
bp – Base pair
CNS - Central nervous system
CPE – Cytopathic effect
DPBS – Dulbecco's phosphate buffered saline
dsDNA – Double-stranded DNA
E.coli – *Escherichia coli*
FBS - Fetal bovine serum
g – Glycoprotein
H/P - Helicase/primase
HIV - Human immunodeficiency virus
HS - Heparan sulfate
HSV – Herpes simplex virus
HSV-1 - Herpes simplex virus type 1
HSV-2 - Herpes simplex virus type 2
HVEM - Herpesvirus entry mediator
ICP - Infected cell protein
INM - Inner nuclear membrane
kPCR – Quantitative polymerase chain reaction
LAT - Latency-associated transcripts
MEM – Minimum essential medium
MOI - Multiplicity of infection
ONM - Outer nuclear membrane
p.i.- Post-infection
PCR - Polymerase chain reaction
pPCR - Amplified PCR product
Primer-F – Forward primer
Primer-R – Reverse primer
RNase – Ribonuclease
rpm – Rotations (revolutions) per minute
RT-PCR – Real-time polymerase chain reaction
STI - Sexually transmitted infection
TG - Trigeminal ganglia
TGN- Trans-Golgi network
U_L – Unique long
U_S – Unique short
VP - Virion proteins

1. Introduction

Herpes simplex viruses (HSV) are important human pathogens that cause disease on a variety of different tissues. As members of the *Herpesviridae* family, they comprise four major components: (i) a core containing a linear double-stranded DNA (dsDNA) molecule (Pellet *et al.*, 2003); (ii) an icosahedral capsid surrounding the core with 162 capsomers (Kukhanova *et al.*, 2014); (iii) an amorphous structure asymmetrically distributed around the capsid designated tegument; and (iv) a host-derived lipid envelope with embedded viral glycoproteins on its surface (Kukhanova *et al.*, 2014). Based on their biological properties, HSV can be further placed in the *alphaherpesviridae* subfamily due to their variable host range, short reproductive cycle, rapid spread in culture and ability to destroy infected cells (Wagner *et al.*, 1997).

Like other herpesviruses, HSV have the ability to remain latent in the host after a primary infection. During latency, the genome acquires a “dormant” state as a circular episome within cells and persists for the lifetime of the infected individual, evading detection by the immune system. Reactivation from latency is often induced by internal/external stimuli leading to productive infection and recurrence of disease (Boehmer *et al.*, 2003, Nicoll *et al.*, 2012).

HSV can be divided into two sub-types, herpes simplex virus type 1 (HSV-1) mostly associated with epithelial cells of the skin and mucosa near the mouth; and herpes simplex virus type 2 (HSV-2), more related to genitalia (Stevens *et al.*, 1971, Singh *et al.*, 2005, Palmer, 2010).

1.1. Transmission, Clinical Manifestations and Prevention/Therapy

HSV transmission occurs by intimate contact with an infected individual and depends on the direct exposure of infectious mucous membranes or abraded skin with the virus, as infected individuals shed it mainly through saliva, tears and genital secretions (Chilukuri *et al.*, 2003, Beauman, 2005, Lee, 2008). HSV-1 and HSV-2 are usually transmitted through different routes of infection, affecting different areas of the body, although the signs and symptoms can overlap (Whitley *et al.*, 2001, Pellet *et al.*, 2003, Roizman *et al.*, 2003). Primary infection by both HSV has, in general, a more severe symptomatology than recurrent infections, leading to the establishment of long-term latency after the infection of sensory nerve endings (Chilukuri *et al.*, 2003, Lee, 2008). Depending on whether the immune system has been compromised, HSV infections can have more severe consequences.

Regarding HSV-1, the most common sites of infection are the skin and mucosal membranes. Oro-facial lesions are characterized by the development of vesicles at the border of the lip (Figure 1.1A) that progress to a pustular or ulcerative state within 3 days. The infection is completely healed in 8 to 10 days; however, viral shedding continues for 3 to 5 days after the lesions have healed (Esmann, 2001, Sciubba, 2003). Ocular lesions (Figure 1.1B) caused by HSV-1 are linked to a variety of ocular complications, being one of the leading causes of corneal blindness and keratoconjunctivitis (Whitley *et al.*, 1998, Rudnick *et al.*, 2002).

On the other hand, HSV-2 infections are more associated with genital herpetic lesions and are currently one of the most prevalent sexually transmitted infections (STIs) worldwide (Smith *et al.*, 2002). After acquisition of infection, macules and papules, followed by vesicles, pustules and ulcers appear

within a few days (Figure 1.1C), for a period that can last up to 6 weeks. Consequences in men are rare, but women can develop serious complications including aseptic meningitis or urinary retention. Primary infections can be associated with fever, dysuria, localized inguinal adenopathy, malaise and headaches (Whitley *et al.*, 2001, Beauman, 2005). Over the past few years, there has been an increased consciousness on genital herpes due to the discovery of its association with the risk of human immunodeficiency virus (HIV) acquisition. The interactions between HSV-2 and HIV may result in a more efficient HIV transmission and in an increase in its replication rate and shedding during a HSV reactivation. The relationship between HSV-2 and HIV seems to be reciprocal, since HIV infections also increase HSV-2 reactivation and probably its acquirement (Beauman, 2005, Mayaud *et al.*, 2008). Educational efforts must be developed for those at greater risk to prevent virus transmission: the use of condoms, for instance, should be promoted, as its use significantly decreases the probability of acquiring STIs.

Neonatal HSV infections are also a very important matter, as they can result in serious morbidity and mortality (Rudnick *et al.*, 2002). Neonate infections can occur *in utero* (5%), *intrapartum* (85-90%) or postnatally (5-10%) (Straface *et al.*, 2012). Infections are usually symptomatic, with sores appearing in the skin, eyes and mouth (Figure 1.1D), and the possibility to affect multiple organs, leading to the baby's death. Most of these infections are due to HSV-2, but 15 to 30% are found to be caused by HSV-1 genital infections (Nahmias, 1970, Rudnick *et al.*, 2002, Lee, 2008).

Additionally, both HSV can infect the central nervous system (CNS) and cause diseases such as encephalitis and meningitis, being one of the most common causes of fatal sporadic encephalitis in humans. Patients may experience fever, malaise, headaches and personality fluctuations. The mortality among untreated patients exceeds 70%, decreasing in treated patients to 19%. However, more than 50% of the patients who survive are left with moderate or severe neuropsychiatric sequels, as only 2.5% of the patients who survive regain normal neurological function (Whitley *et al.*, 1998, Whitley *et al.*, 2001, Meyding-Lamadé *et al.*, 2012).

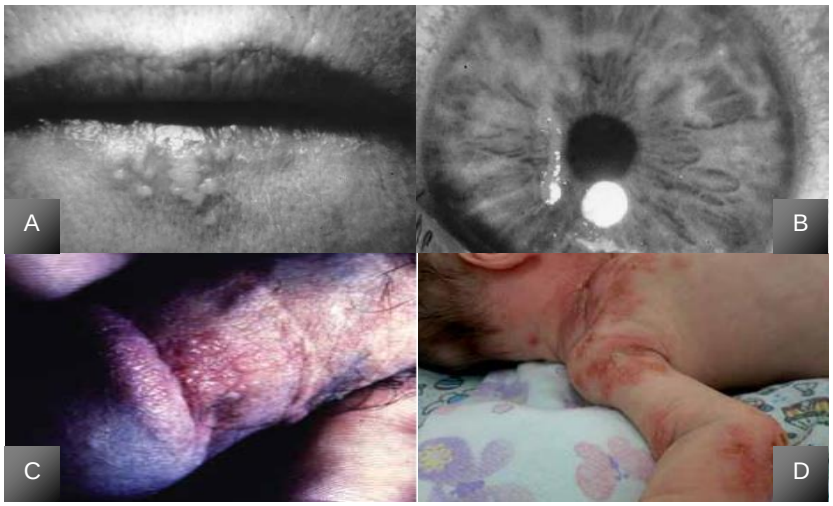

Figure 1.1: Herpesvirus induced lesions.

[A] Oral herpes; **[B]** Ocular herpes; **[C]** Genital Herpes; **[D]** Neonatal herpes.

[A][B] (Pellet *et al.*, 2003, Roizman *et al.*, 2003); [C] (Beauman, 2005); [D] (Bittencourt *et al.*, 2016)

Despite an increasing awareness regarding both HSV-1 and HSV-2 infections, many cases remain undiagnosed, as they are usually asymptomatic (silent transmission to partners or to the neonate) or unrecognized, when symptomatic infections are present in an unusual or atypical way, making the diagnosis harder (Roizman *et al.*, 2003).

Currently, there are several systemic antiviral agents against HSV. The most effective treatment is acyclovir or its prodrugs valacyclovir and famciclovir (Chilukuri *et al.*, 2003, Pellet *et al.*, 2003, Lee, 2008, Martinez *et al.*, 2008). Even though these drugs can treat herpes disease, they cannot prevent reactivations. In addition, prolonged prophylaxis and treatment can result in the development of drug resistance, particularly in immunocompromised patients (Bacon *et al.*, 2003).

1.2. Epidemiology

HSV infections occur worldwide, without seasonal variation. Despite the fact that infections caused by HSV are a serious health problem worldwide, few updated epidemiological data exist, with the most recent ones dating from 2012. Nevertheless, it is known that the prevalence of both HSV infections varies according to the subject's age, country, regions and population subgroups (Smith *et al.*, 2002).

Regarding HSV-1, it has been estimated that 3.7 billion people under the age of 49 are globally infected with this subtype (Looker *et al.*, 2015a). This prevalence was clearly higher in Africa, South-East Asia and Western Pacific than for Europe, Americas and Western Mediterranean. However, a different scenario was seen for the HSV-1 genital infections, which seem to be globally increasing. Of the 3.7 billion prevalent cases, ~140 million correspond to prevalent genital HSV-1 infections, primarily in the Americas, Europe and Western Pacific (Looker *et al.*, 2015a).

Concerning HSV-2, the estimated worldwide prevalence among people between the ages of 15 and 49 was 417 million (Looker *et al.*, 2015b). Prevalence was higher in Africa (31.5%) and generally higher in females compared to males (14.8% vs. 8%). This difference is due to the fact that women have greater biological susceptibility to HSV-2, although different patterns of sexual behavior between the sexes can expose women to a higher risk of infection. Estimates also indicate that ~ 23 million new cases are diagnosed every year (Looker *et al.*, 2008)

Neonatal HSV has an estimated incidence of around one in 2000 to 5000 births *per* year, although in some areas there can be as many as one neonatal infection in 1500 deliveries. This incidence is directly related to the seroprevalence of HSV-2 (Looker *et al.*, 2015a).

1.3. Virion structure and Genomic organization

The mature infectious HSV virion has four distinct structural components: the dsDNA genome is enclosed within an icosahedral capsid, surrounded by a proteinaceous tegument and a host-derived lipid envelope (Figure 1.2).

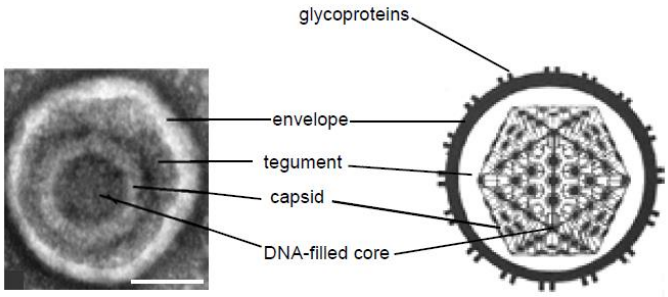

Figure 1.2: The HSV-1 virion.

Electron micrograph of a negatively stained HSV-1 virion and a cartoon representation showing the components comprising the virion. Adapted from Roizman *et al.*, 2003.

1.3.1. Central core and Genome

The HSV core contains a dsDNA molecule, with approximately 152 to 155 kilo base-pairs (kbp) and a 68.3%-70.4% G+C content (Szpara *et al.*, 2014, Kolb *et al.*, 2015). The genome comprises two covalently linked components, L (long) and S (short), with unique sequences U_L (107.09 kbp) and U_S (12 kbp), respectively, flanked by large inverted repeats (Figure 1.3). The UL and US units of the genome can invert relative to one another, producing four different types of DNA molecules (Kukhanova *et al.*, 2014). The genes of the long and short unique sequences are designated *UL1* to *UL56*, and *US1* to *US12*, respectively. UL and US encode about 70 proteins, designated virion proteins (VP) and infected cell proteins (ICP) (Dolan *et al.*, 1998, Palmer, 2010).

Figure 1.3: HSV genome structure.

The long component of the genome (U_L) is flanked by inverted repeats designated as **a** (black) and **b** (dark grey), and **b'a';** the short component (U_S) is flanked by **a'c'** and **ca** sequences. Adapted from Kukhanova *et al.*, 2014.

The genetic maps of both HSV genomes confirms the co-linearity and shows an overall identity of 83% (Roizman *et al.*, 2003). Nevertheless, the two genomes differ in the location of endonuclease cleavage sites in their genomic DNAs, in the apparent sizes of the encoded proteins, as well as in some glycoproteins that are unique for each virus (Roizman *et al.*, 2003, Szpara *et al.*, 2014).

1.3.2. Capsid

During an HSV infection, the capsid plays a central role in delivering the genome of the virus into the host cell nucleus. The capsid, where DNA is stored, consists mainly of four proteins: VP5 (coded by the UL19 gene), VP19C (UL38), VP23 (UL18) and VP26 (UL35). VP5 is the major capsid protein and is present in both pentons, forming the vertices, and hexons, forming the faces (Baines, 2011). VP26 is present as a ring on top of the VP5 subunits of each hexon (Zhou *et al.*, 1995), whereas triplexes made of one VP19C and two VP23 molecules link adjacent capsomers. One of the vertices is unique, consisting of 12 copies of the portal protein UL6 through which viral DNA is sent into the nucleus (Bowman *et al.*, 2003, Roizman *et al.*, 2003, Brown *et al.*, 2011).

Four types of capsids can be isolated from infected cells. First, spherical procapsids are formed, containing the internal scaffold. During infection, the maturation of procapsids gives rise to A-, B- and C-capsids. A-capsids lack both scaffold proteins and viral DNA, and are incapable of maturation; B-capsids have scaffold proteins and are thought to be in an early stage of viral assembly; C-capsids contain the viral genome and can become infectious virions (Gibson *et al.*, 1972, Sheaffer *et al.*, 2001, Palmer, 2010, Tandon *et al.*, 2015).

1.3.3. Tegument

The tegument occupies the space between the capsid and the envelope, and can be divided in inner tegument, which is tightly bound to the capsid, and outer tegument, connected to the viral envelope (Scrima *et al.*, 2015). It occupies about two thirds of the volume enclosed within the virion (Grunewald *et al.*, 2003) and is made of, at least, 20 different proteins. The tegument functions as a delivery compartment for proteins during the early course of infection and participates in virion assembly (Lee, 2008).

1.3.4. Envelope

The outer layer of the HSV virion is a host-derived envelope, consisting in a lipid bilayer with around 13 virally encoded glycoproteins (g) embedded in it. HSV glycoproteins have roles in attachment and entry into the host cell, even though the function of each glycoprotein varies according to the overall pathogenesis and immune evasion strategy of the virus (Kukhanova *et al.*, 2014). Nevertheless, it is known that gB, gC, gD, gH and gL are essential for the infection process (Reske *et al.*, 2007).

1.4. HSV life cycle

HSV is thought to have a relatively short life cycle of about 15 to 24 hours (Jenkins *et al.*, 1996, Lehman *et al.*, 1999, Roizman *et al.*, 2003, Schiffer *et al.*, 2013) that can be divided in six major steps: (i) entry into the host cell, (ii) viral gene expression, (iii) viral DNA replication, (iv) viral maturation, (v) viral egress and (vi) latency.

1.4.1. Entry into the host cell

HSV has two ways of getting into the host cell: endocytosis, not yet fully understood; and membrane fusion, a much well known and studied process (Figure 1.4) (Heldwein *et al.*, 2008).

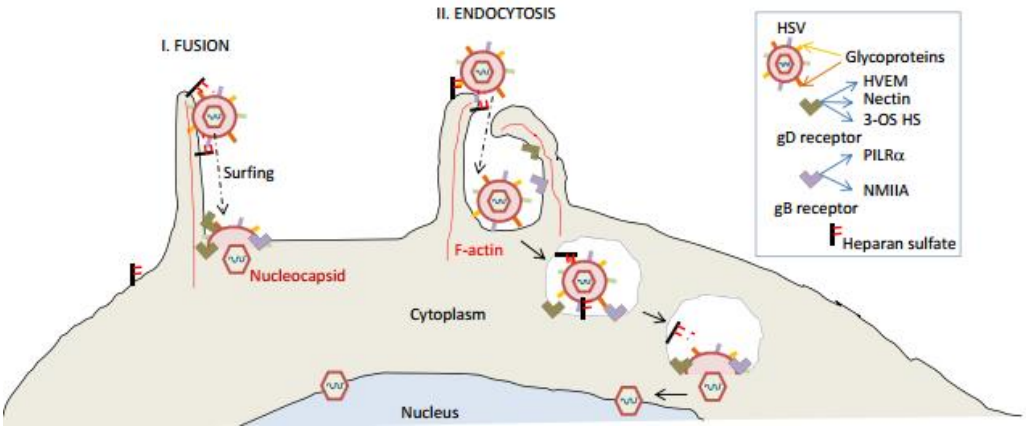

Figure 1.4: Pathways of HSV entry into the cell.

Two major entry pathways are known for HSV entry: (I) entry by viral envelope fusion at the plasma membrane and (II) endocytosis. Both processes lead to the delivery of the HSV genome into the host cell (Salameh *et al.*, 2012).

Initial attachment/entry is mediated via gC (or gB, in case gC is unavailable), that binds to the cell surface's glycosaminoglycans, in particular heparan sulfate (HS) (Campadelli-Fiume *et al.*, 2012). Afterwards, gD interacts with one of the three entry receptors: (i) the herpesvirus entry mediator (HVEM), a component of T and B-lymphocytes, epithelial cells and fibroblasts; (ii) both Nectin-1 and Nectin-2, members of the immunoglobulin family, expressed in human tissues including epithelial cells, fibroblasts and neurons, or (iii) the 3-O sulfated heparan sulfate (3-OS-HS), a polysaccharide present in endothelial cells (Figure 1.5) (Spear, 2004, Salameh *et al.*, 2012, Kukhanova *et al.*, 2014). Despite structural disparities and different interactions with gD, the binding to one of the three receptors described above leads to the same endpoint: membrane fusion (Heldwein *et al.*, 2008, Gianni *et al.*, 2009, Kukhanova *et al.*, 2014).

The next step requires gB and the heterodimer gH/gL (Figure 1.5), resulting in the release of the capsid and of approximately 20 tegument proteins into the cell's cytoplasm. The capsids and several tegument proteins are transported through the cell to the nucleus via microtubules, mediated by the retrograde motor dynein (Döhner *et al.*, 2002, Palmer, 2010, Kukhanova *et al.*, 2014). Once the capsids have reached the proximity of the nucleus, they dock at the nuclear pore, releasing the viral genome through the UL6 portal (Roizman *et al.*, 2003, Kukhanova *et al.*, 2014, Fay *et al.*, 2015). Upon entry into the nucleus, viral DNA circularizes within 30 minutes post-infection (p.i.) (Boehmer *et al.*, 2003).

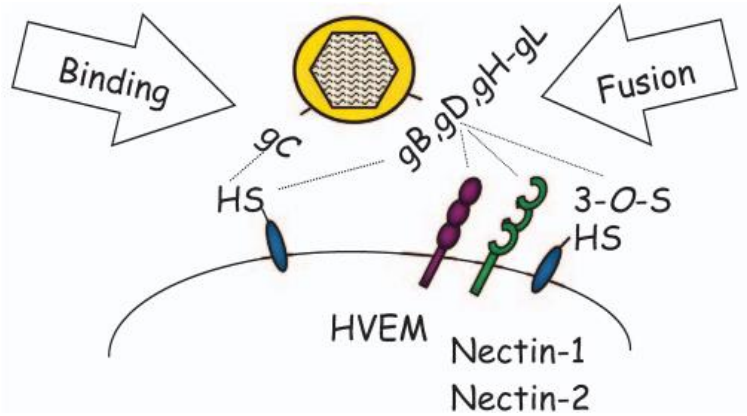

Figure 1.5: Multiple receptors upon HSV entry.

gC mediates the initial attachment of virus particles to HS. The next step involves the interactions between gD with HVEM, Nectin-1/Nectin-2 or 3-OS-HS**,** resulting in membrane fusion, later mediated by the gH-gL heterodimer, resulting in the release of the viral nucleocapsid into the host cell cytoplasm (Spear, 2004).

1.4.2. Viral gene expression

Once the nucleocapsid reaches the nucleus and the viral DNA ejects, transcription begins (Ramachandran, 2003). HSV, as all herpesvirus, has a controlled temporal cascade of gene expression, with three classes of genes, designated α (or IE – immediate early), β (or E – early) and γ (or L – late). All genes are transcribed using the host's RNA polymerase II (Honess *et al.*, 1974, Lee, 2008, Palmer, 2010). The α genes begin to be expressed very soon after viral entry and α proteins reach their peak 2 to 4 hours p.i., encoding proteins involved in the transcription of other viral genes. Transcripts are transported to the cytoplasm and translated into five proteins, being the most important one ICP0. Immediate early proteins accomplish multiple functions and perform dramatic reorganization of cellular processes in the interest of the virus (Boehmer *et al.*, 2003, Kukhanova *et al.*, 2014). β genes are expressed following the accumulation of α proteins, and their expression peaks around 5 to 7 hours p.i. encoding proteins responsible for viral DNA replication, and signaling the onset of viral DNA synthesis, which results in the expression of γ genes. The expression of the later genes typically peaks between 8 and 12 hours p.i., and can be further divided in two sub-classes, γ1 and γ2, depending on their expression kinetics (Figure 1.6) (Honess *et al.*, 1974, Ramachandran, 2003).

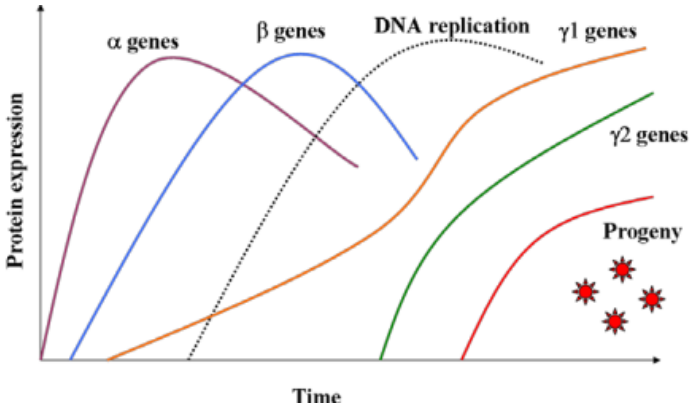

Figure 1.6: General pattern of gene expression during a HSV infection.

The first genes to be expressed are α genes (purple) followed by β genes (blue). Meanwhile, DNA replication begins (dotted line). At this point, γ genes start to be expressed: γ1 (orange) can be expressed prior to DNA replication, and γ2 (green) requires DNA synthesis to be expressed. Once the proteins have accumulated, progeny viruses (red) assemble (Ramachandran, 2003).

1.4.3. Viral DNA Replication

DNA replication takes place after the expression of α and β genes, using the circularized DNA as template. The HSV genome contains three origins of replication (Figure 1.7): *OriS*, present twice in the *c* inverted repeats flanking the US region, and *OriL* located in the middle of the UL region (Weller *et al.*, 2012).

$$a_1\ a_n\ b\text{----------}\ ori_L\text{----------}\ b'\ a_n'\ c'\ ori_S\ \text{-------}\ ori_S\ c\ a_S$$

Figure 1.7: HSV origins of replication.

The figure shows the organization of the HSV genome, with the origins of replication shown as *OriL* and *OriS*. Both *OriS* and *OriL* are located in the promoter-regulatory regions of divergently transcribed genes: *OriL* between genes encoding replication proteins and *OriS* between genes encoding α proteins. Adapted from de Silva *et al.*, 2009.

The DNA is replicated using a virally-encoded replication complex comprising an origin-binding protein UL9; a single stranded DNA-binding protein ICP8 (UL29); the DNA polymerase and DNA polymerase processivity factor, UL30 and UL42, respectively; and the DNA helicase/primase (H/P) complex UL5, UL52 and UL8 (Lehman *et al.*, 1999, Weller *et al.*, 2012).

The first stage of DNA replication involves an origin-UL9-dependent step. Upon DNA circularization, UL9 binds to specific recognition sites in either *OriL* or *OriS* and begins to unwind the viral DNA. UL9 then recruits ICP8, resulting in the recruitment of the helicase-primase heterodimer, followed by the polymerase complex (Figure 1.8). The second stage of replication is UL9-independent, and leads to the formation of longer-than-unit length concatemers, later packaged into procapsids in the form of monomeric units (Whitley *et al.*, 2001, Boehmer *et al.*, 2003, Kukhanova *et al.*, 2014).

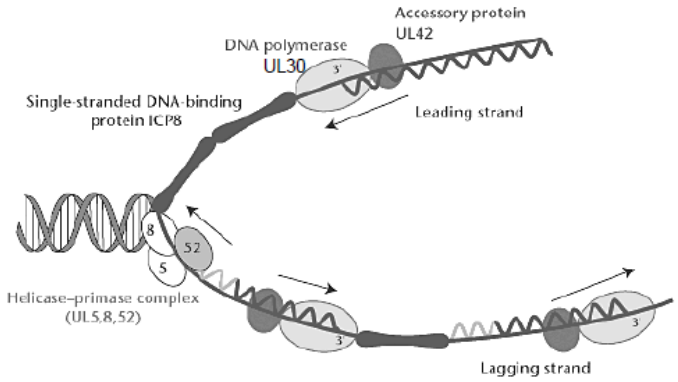

Figure 1.8: Model of HSV DNA replication.

Replication fork model. The H/P complex, made of proteins UL5, UL8 and UL52, unwinds the DNA; the binding protein ICP8 binds to single-stranded template DNA; the polymerase (UL30) and its accessory protein UL42 promote leading and lagging-strand DNA synthesis. Adapted from Crumpacker *et al.*, 2002.

1.4.4. Viral maturation

Following repeated rounds of DNA synthesis, concatemeric genomes accumulate within replication compartments. The synthesis of γ genes, encoding late proteins that include structural proteins, envelope proteins incorporated in nuclear membrane and several other structural and packaging proteins, lead to the assembly of new progeny virions (Lehman *et al.*, 1999). Capsids are initially formed as procapsids with an internal protein scaffold made of UL26 and UL26.5 gene products, which is lost upon DNA packaging. The protease UL26 cleaves itself, generating capsid proteins VP24 and VP21, and UL26.5, generating VP22a (Newcomb *et al.*, 2000, Mettenleiter *et al.*, 2006). Capsid formation also requires the capsid proteins VP5, VP23 and VP19C (Mettenleiter *et al.*, 2009). The procapsids differ from mature capsids in several aspects: while the procapsids are spherical, have a more porous structure with holes between capsomers and have oval hexons, mature capsids (A-, B- or C-) are icosahedral, have a less porous composition and have hexagonal hexons (Newcomb *et al.*, 2000, Mettenleiter *et al.*, 2006). Procapsids transform into mature capsids in a process in which the shell undergoes structural changes (Figure 1.9). Capsid maturation overlaps with viral DNA packaging, resulting in a mature C-capsid containing the viral genome. C-capsids are the only ones able to undergo egress and further maturation (Goshima *et al.*, 2000, Sheaffer *et al.*, 2001, Bucks *et al.*, 2007).

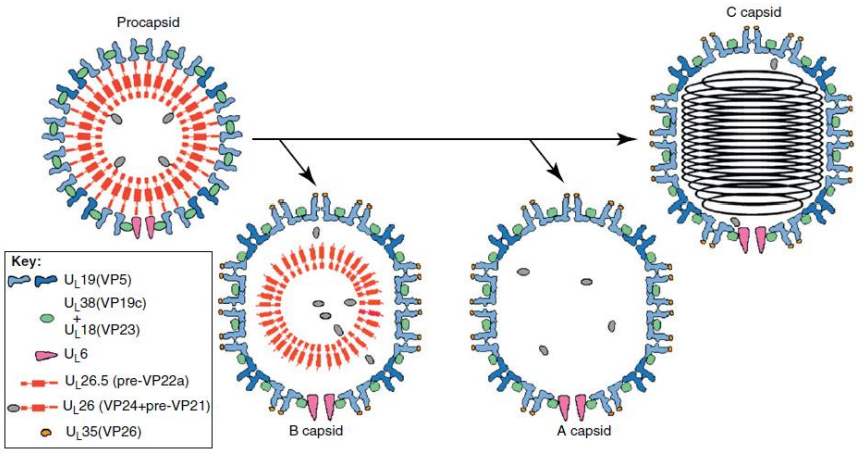

Figure 1.9: HSV capsid maturation.

The spherical procapsid is the precursor of all other capsid types. It is made primarily of VP5 pentons (dark blue) and hexons (light blue) linked by triplexes (green), with 12 copies of UL6 that will eventually form the portal. The inner scaffold shell is lost or degraded in A capsids, retained in B capsids, and replaced with DNA in C capsids. Adapted from Baines, 2011.

1.4.5. Viral egress

Successful encapsidation of the viral genome is followed by budding through the modified inner nuclear membrane (INM) into the perinuclear space to acquire the primary envelop and continue the maturation process (Kukhanova *et al.*, 2014). Several models have been proposed over the years to explain the exact egress pathways; however, the most exact one is the envelopment-deenvelopment model. According to this, capsids dispersed in the nucleus approach and attach the INM, through intranuclear movement via nuclear actin filaments, induced by HSV infection (Mettenleiter *et al.*, 2009). Proteins UL31 and UL34 are crucial for this process, since the UL31/UL34 nuclear envelopment complex induces conformational changes in the nuclear lamina. This disruption of the lamina allows the capsids to bud into the perinuclear space gaining a primary tegument and envelope (Figure 1.10A) (Newcomb *et al.*, 2006, Kukhanova *et al.*, 2014).

Next, nucleocapsids undergo a de-envelopment process, by fusing with the outer nuclear membrane (ONM), resulting in the loss of the primary envelope and nucleocapsid release into the cytoplasm, for continuing maturation (Figure 1.10B) (Roizman *et al.*, 2003, Mettenleiter *et al.*, 2006, Mettenleiter *et al.*, 2009).

After nuclear egress, the nucleocapsids have to acquire tegument proteins and the final (secondary) envelope in order to exit the cell (Mettenleiter *et al.*, 2009). This process occurs predominantly in the cytoplasm, and is controlled by a complex network of protein-protein interactions (Owen *et al.*, 2015). HSV nucleocapsids make their way toward cytoplasmic vesicles derived from the trans-Golgi Network (TGN) to reacquire their envelop (Figure 1.10C).

Currently, little is known about the mechanism by which mature virions are released from cells, but it is thought that these viruses use proteins from the host cell's secretory pathway to facilitate egress at the plasma membrane. The virus-containing secretory vesicles move to the plasma membrane, where

they fuse and release mature virions, by exocytosis, resulting in the death of the host cell (Figure 1.10D) (Mingo *et al.*, 2012).

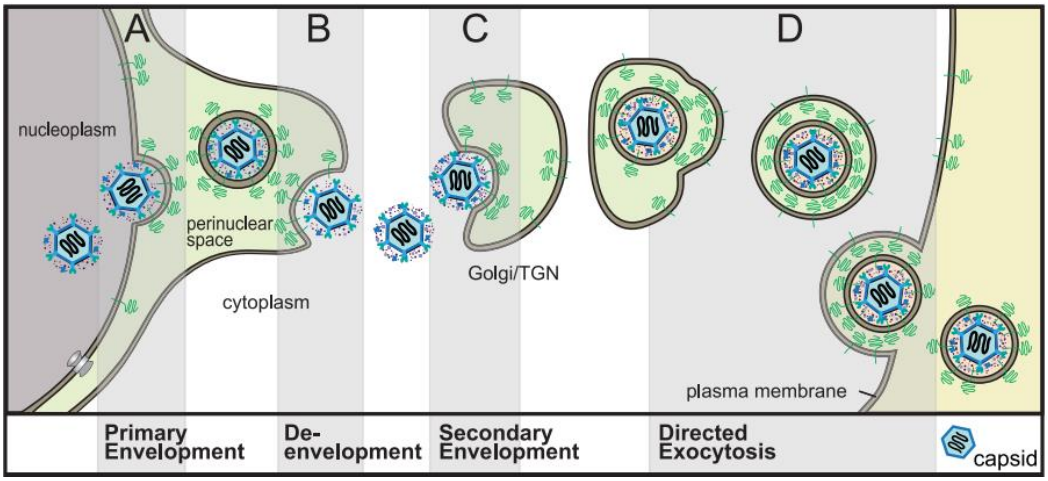

Figure 1.10: HSV viral egress.

[A] Primary Envelopment - After capsids are formed in the nucleus, they bud into the INM to form an enveloped particle in the perinuclear space;

[B] De-envelopment - HSV particles reside in the perinuclear space. HSV glycoproteins gB and gH/gL mediate fusion of the viral envelope with the ONM;

[C] Secondary Envelopment - In the cytosol, capsids coated with numerous tegument proteins bind onto the surface of the TGN that contains HSV glycoproteins. Interactions between all of these proteins promote envelopment;

[D] Egress - Virions are transported to cell surface in exocytic vesicles, leading to the death of the host cell. Adapted from Johnson *et al.*, 2011).

1.4.6. Latency-Reactivation Cycle

Herpesvirus have the ability to establish latency, one of the most intellectually challenging aspects of HSV biology (Stevens *et al.*, 1971). Despite a vigorous immune response during an infection, HSV establishes latency in sensory neurons, typically trigeminal ganglia for HSV-1 and sacral ganglia for HSV-2. Remarkably, up to 40% of sensory neurons can be latently infected (Kramer *et al.*, 1998, Perng *et al.*, 2010, Nozawa *et al.*, 2014).

The latency-reactivation cycle can be divided into three major steps: (i) establishment, (ii) maintenance, and (iii) reactivation. Establishment of latency includes the entry of the viral genome into a sensory neuron, through retrograde axonal transport (Figure 1.11). Viral gene expression is silenced with the exception of one set of transcripts that continue to be expressed known as latency-associated transcripts (LAT) (Nicoll *et al.*, 2012, Ma *et al.*, 2014). Maintenance of latency is a phase that lasts as long as the host lives, and is defined as a period when infectious genes are not detected, but LATs continue to be expressed. The full length 8.3 kbp LAT is transcribed from the latency associated promoter and is sliced, giving rise to two stable 2.0 kb and 1.5 kb introns (Nicoll *et al.*, 2012, Kukhanova *et al.*, 2014). These two LAT forms accumulate in the nuclei of latently infected neurons and are directly anti-sense to HSV lytic protein ICP0, preventing viral gene transcription through a slow and multistep

process that results in the decrease of α genes expression (Jackson *et al.*, 2003). During latency, the viral genome circularizes and is maintained as an episome within the nucleus (Ramachandran, 2003). In Humans, latency is maintained throughout the host's life, indicating that a well-conceived strategy exists, allowing periodic reactivation, while maintaining the viral genome in sensory neurons. Reactivation from latency is initiated by an external stimulus, such as stress or immunosuppression, culminating in viral gene expression. Clinically, depending on the host immune status, reactivation can be symptomatic, where the virus can be detected in peripheral tissues and disease is recognized, resulting in lesions, or asymptomatic, where the virus can be laboratory detected but signs of disease are unrecognized. In both cases, the virus is carried by anterograde axonal transport (Figure 1.11) to peripheral tissues through the motor protein kinesin, usually to cells at, or near the site of initial infection. Reactivation leads to viral expression and generation of progeny virions (Perng *et al.*, 2010).

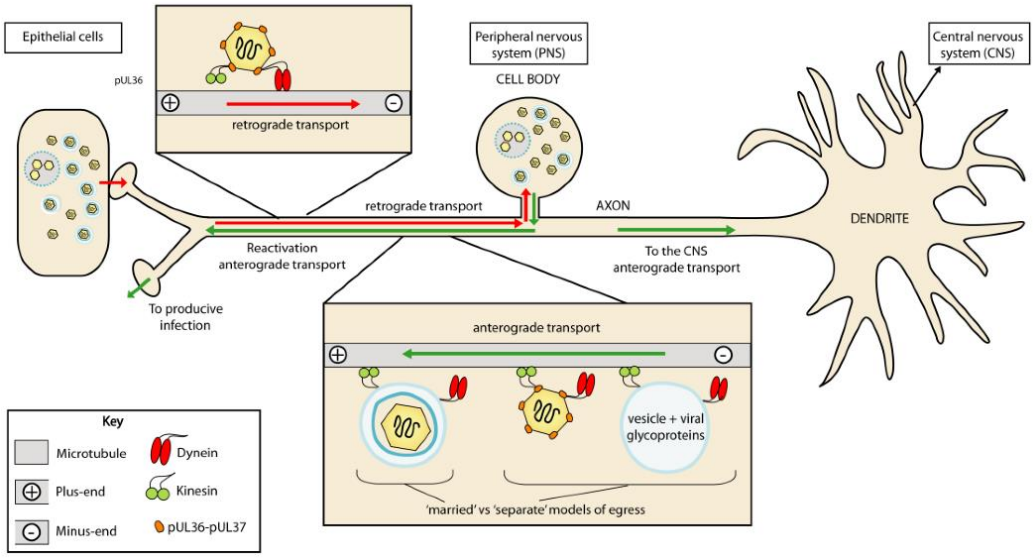

Figure 1.11: Neural trafficking during latency-reactivation cycle.

HSV establishes latent infection in the nuclei of peripheral ganglia, following retrograde transport along microtubules, through the dynein transport protein. Reactivation results in the production of new virions that undergo anterograde transport back to peripheral tissues with the transport protein kinesin. Adapted from Owen *et al.*, 2015.

1.5. Scope of the Thesis

HSV infects a variety of host cells, including lymphocytes, epithelial cells, fibroblasts, and neurons (Connolly *et al.*, 2011). Although there are multiple studies that try to evaluate the infection patterns of HSV, including among sub-types, none of them is conclusive and reproducible, being even sometimes contradictory (Docherty *et al.*, 1971, Tada *et al.*, 1977, Nguyen *et al.*, 2005, Aguilar *et al.*, 2006). For instance, even though HSV is considered to have a relatively short life cycle when compared with other viruses, there doesn't seem to be a consensus regarding the duration of the infectious process, as cycles ranging from 15 to 24 hours can be currently found throughout the literature (Jenkins *et al.*, 1996, Lehman *et al.*, 1999, Roizman *et al.*, 2003, Schiffer *et al.*, 2013). Moreover, it is also not known whether HSV-1 or HSV-2 strains display different infectious patterns and virulence depending on the host

infected tissue (oro-facial tissue versus genitalia), even though it is known that HSV-1 genital reactivations appear to be less common and timely shorter than those of HSV-2. Indeed, as seen for other human pathogens (Nunes *et al.*, 2013, Martines *et al.*, 2015), the observed cellular tropism doesn't seem to be straight to a particular HSV type. Differences in viral evolutionary dynamics, such as evolution rates, can explain why certain viruses have the capacity to adapt to new host species, increase in virulence, or develop resistance to antivirals (Hicks *et al.*, 2014).

In order to contribute for this knowledge, the scope of this thesis was to evaluate the life cycle of various genital HSV-1 and HSV-2 clinical isolates with different viral loads in distinct host cell lines, giving special focus to the invasion process. Considering that there has been an increase in the number of cases of genital herpes caused by HSV-1, especially among the younger population, it is of utmost importance to understand whether HSV-1 in the genitalia replicates the same way as it does in mouth sores (not evaluated in the present study), or if it has an alternative route of infection that may be similar to that of HSV-2. In particular, understanding whether capacities of infections, replication rates, and progenies depend on the genital HSV sub-type/strain or on the infected cell line is a mandatory step for the understanding of the pathogenesis of human herpes infections and may be important for the development of a more effective antiviral chemotherapy.

To achieve robust and reliable conclusions, four genital HSV samples isolated from genital swabs, two HSV-1 and two HSV-2, were used in the present study, as well as three host cell lines with different phenotypic and molecular characteristics. Hence, specific objectives of these assays were:

1) To assess whether genital infections caused by HSV-1 and HSV-2 have the same molecular characteristics, in a particular cell line;

2) To test if both HSV display the same infection capacity in all three cell lines tested;

3) To measure whether there is a viral saturation in a HSV infection in the three cell lines;

4) To determine the duration of the HSV-1 and HSV-2 life cycle;

5) To determine when does DNA replication begin;

6) To assess when viral progeny begins to be generated.

2. Materials and Methods

2.1. Biological samples

The viruses used in the present study were obtained from ulcer and genital/urethral swabs of four patients suspected of having a HSV infection, from a Sexually Transmitted Diseases Outpatient Clinic. The viral swabs (with viral transport medium) were sent for confirmation of diagnosis to the National Reference Laboratory of Herpes simplex virus, Cytomegalovirus and Parvovirus B19 of the Portuguese National Institute of Health (INSA), in Lisbon, and treated according to laboratory protocol. After swab agitation and content filtration with a 0.45µm filter, DNA was extracted using the automatic nucleic acid extractor NucliSENS® EasyMag® (BioMérieux). HSV-1 and HSV-2 DNA was quantified with a commercial real-time PCR (RT-PCR) kit (HSV1 HSV2 VZV R-gene®, ARGENE®, BioMérieux), that targets a 142 bp fragment of the US7 gene from HSV-1 and a 177 bp fragment of the US2 gene from HSV-2. PCR reactions were carried out with the amplification platform ABI PRISM® 7500 (Applied Biosystems®). Positive results were reported as copies/mL, taking into consideration sample extracted volume, final elution volume and DNA volume used in the amplification reaction.

The epidemiological, laboratory and clinical data of the selected clinical isolates are described in Table 2.1:

Table 2.1: Epidemiological, laboratory and clinical data.

Clinical isolates	Virus	Patients information				Viral Load copies/mL
		Gender	Age	Episode	Location	
A	HSV-1	Female	22	Primary infection	Vulva, perineum	46 058 248
B	HSV-1	Female	22	Symptomatic reactivation	Vulva	87 474 493
C	HSV-2	Male	32	First symptomatic episode, but not primary infection	Penis	526 335 906
D	HSV-2	Female	24	--- Not available ---	Vulva	302

2.2. Cell line handling and maintenance

The present experimental work was performed using three different adherent epithelial cell lines that, due to their susceptibility to a wide range of hosts, are usually used in virology studies, in particular for HSV: Vero (ATCC® CCL-81™) and Vero E6 (ATCC® CRL-1586™) from the kidney of the African Green monkey, and HeLa229 (ATCC® CCL2.1™) from a cervix adenocarcinoma of a 31-year old black woman. Vero E6 cells differ from regular Vero cells since they show some degree of contact inhibition, being suitable for supporting the growth of slowly replicating viruses. All cell lines were purchased from the American Type Culture Collection.

Each cell line was grown in 175 cm^3 tissue culture flasks (T175; Sarstedt) with Dulbecco's Minimum Essential Medium (MEM 1x + GlutaMAX™; Gibco, USA) supplemented with 10% fetal bovine serum (FBS; Gibco, USA). For both Vero and Vero E6 cells, the medium was further complemented with 1% HEPES buffer solution 1M (Gibco, USA), 1% Non-Essential Amino Acids (NEAA 100x; Gibco, USA) and 0,2% Antibiotic Mixture (PSN 100x; Gibco, USA), while for HeLa229 cells, Gentamicin (50 mg/mL; Gibco, USA) and Fungizone (250 µg/mL; Gibco, USA) were added. Cell cultures were incubated in a CO_2 incubator (Binder) at 37ºC with a 5% CO_2 atmosphere, and cellular growth was followed by observing cultures under an inverted optic microscope (Leica DMIL LED).

In order to produce sufficient cellular stocks for all assays, each cell culture was subjected to continuous passages whenever a 90% confluent cell monolayer was reached. Briefly, after the medium was removed and the cells washed twice with 10 mL of Phosphate Buffered Saline (DPBS 1x; Gibco, USA), 5 mL of trypsin (0.5% Trypsin-EDTA 10x; Gibco, USA) were added to the flask, following an incubation of 5 minutes in the CO_2 incubator, in order to detach the cells. After that time, the cells were ressuspended and added to a new flask with fresh medium.

2.3. Preliminary assays

For each cell line and HSV isolate, preliminary assays were performed to determine the optimal cellular concentration, culture conditions and viral loads to be used for the subsequent quantification assays. The inoculation process was also evaluated in order to better mimic an *in vivo* HSV infection.

2.3.1. Cell counting

For each cell line, in order to ensure that HSV inoculation occurred on a 90% confluent cell monolayer, cell density was verified 24 hours before the assays, using the trypan blue method on a hemocytometer (Spencer-Buffalo, USA). Briefly, confluent T175 culture flasks were treated as stated in step 2.2 and resuspended; then, 50 µL of the cell suspension were added to 200 µL of Hanks' Balanced Salt Solution (HBSS 1x; Gibco, USA). Following vortex agitation (PV-1 Vortex Mixer, Grant), 50 µL of this solution were added to 50 µL of trypan blue (Sigma), which stains dead cells. Finally, 10 µL of this solution were placed in each of the two hemocytometer chambers, and the number of viable cells (not stained by the trypan blue) were counted under the microscope (Leica DM IL LED). Cell density was determined through equation (1):

$$(1)\ \left[\frac{Number\ of\ cells}{mL}\right] = \left(\frac{\sum Cells\ per\ quadrant}{4}\right) \text{ x } 10^4 \textit{ (Chamber volume x dilution factor)}$$

2.3.2. Culture conditions

Considering that the success of any microbial infection depends, among other factors, on the availability of nutrients in the medium, the optimal FBS quantity to be added to each cell culture was determined, in order to guarantee, not only that a confluent monolayer was achieved at the time for the experiments, but also that this monolayer was stable enough to support the entire period of a viral infection. Basically, suspensions of each cellular culture were seeded into two 24-well plates, with half of the wells containing 4% FBS, while the other half had 10% FBS (Figure 2.1). The plates were then

placed in a CO_2 incubator (Binder) at 37ºC with a 5% CO_2 atmosphere, one for 48h and the other for 72h. Cellular growth was evaluated by both visual assessment on an inverted optical microscope and cell counting.

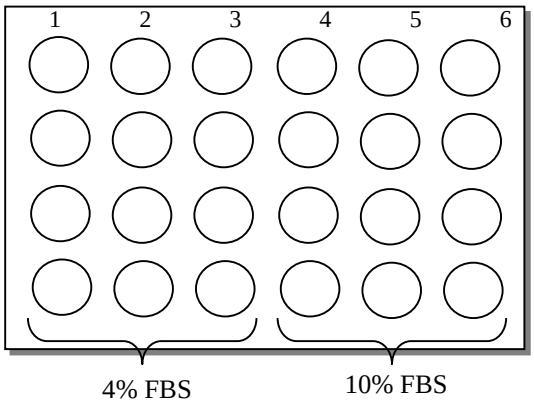

Figure 2.1: Nutrient availability assay plate scheme.

2.3.3. Viral stocks

For each HSV under evaluation, viral stocks were produced by inoculating 100% confluent Vero cells monolayers. Infected cells were incubated at 37ºC with a 5% CO_2 atmosphere for 1-4 days, until they showed cytopathic effect (CPE), i.e., severe morphological alterations in infected cells and lack of adherence (Figure 2.2).

Culture flasks were frozen and defrozen in order to detach all cells from the walls of the flask. Virus suspensions were well homogenized, aliquoted into 2 mL tubes and stored at -80ºC, until use. In average, a total of 100 mL of stock were produced for each virus. For all four viral stocks, two aliquots were randomly selected and subjected to DNA extraction followed by subsequent absolute quantification by RT-PCR, as described in 2.1.

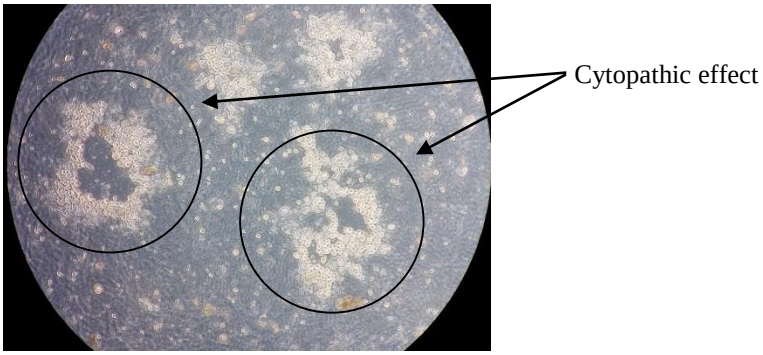

Figure 2.2: CPE on Vero cells after a one-day incubation with a HSV-2 virus.

The final viral loads, after viral stock production, and based on which further calculations were made (for step 2.4) are presented in table 2.2.

Table 2.2: Final viral charges, after viral stock production.

Clinical isolate	Virus	Final viral charge copies/µL
A	HSV-1	6.05×10^6
B	HSV-1	2.76×10^6
C	HSV-2	2.16×10^7
D	HSV-2	3.68×10^{12}

2.3.4. Inoculation conditions

In order to better mimic the HSV infection *in vivo*, two different *in vitro* inoculation conditions were tested in parallel: one involved centrifugation and the other agitation. To achieve robust conclusions, two HSV-2 clinical isolates, with distinct viral loads (3-fold difference) were used. Briefly, quadruplicate 24-well plates with confluent Vero cells monolayers were prepared, after adding coverslips to two sets of plates. Inoculations were performed by adding 200 µL of each HSV-2 virus *per* well to 1/3 of the wells/plate (Figure 2.3).

After inoculation, two sets of plates (one with and another without coverslips) were centrifuged at 700g for 45 min, at 4ºC (Centrifuge 5810 R, Eppendorf), in order to mechanically promote only viral attachment to the host cells. At 4ºC, no cellular metabolism occurs, preventing any viral entry. The entry process is then synchronized, ensuring that attached viruses will later enter (at a higher temperature) at the same time. The other two plates (with and without coverslips) were subjected to agitation at 20 rpm for 1 hour (Rocking Platform VWR®), at 37ºC (Memmert), allowing the viruses to attach and possibly enter host cells in a less artificial way, at different rates. At the end of both processes, inoculum and dead cells were removed, and 1 mL of new media complemented with 4% FBS was added, thus accounting time-point “0”.

Plates were then incubated for ~ 30 hours at 37ºC with a 5% CO_2 atmosphere. Infection was followed at different time-points (4h, 7h, 9h, 13h, 18h, 23h and 29h p.i.) in order to evaluate the putative HSV growth curve. The plates without coverslips were subjected to RT-PCR absolute quantification (Figure 2.3A) for determining viral load at each time-point, while the others were used for monoclonal antibody staining to monitor eventual changes at a cellular level (Figure 2.3B).

Regarding RT-PCR, the wells were scratched at the indicated time-points of infection and kept at -20ºC until use. Extractions were later performed using the QIAamp® DNA Blood Mini Kit (Qiagen), according to the manufacturer’s instructions. The HSV-2 DNA was amplified and quantified using the HSV1/HSV2/VZV R-gene®” ARGENE® kit, as instructed, using the amplification platform ABIPRISM 7500 (Applied Biosystem). For immunofluorescence, the medium was removed at each time-point, washed twice with 1 mL of DPBS and fixed with methanol. After a 10 min air-dry, DPX (Fluka, BioChemika) was added for the coverslip to adhere to a slide. 50 µL of the monoclonal antibody specific for HSV-2 (Pathfinder™ HSV 1/2, Biorad) were added to the coverslips, following a 30 min incubation period in a wet chamber and agitation on a rocking platform (Rocking Platform VWR®). After washing

the slides with DPBS, 50 µL of Mounting Medium were added. All slides were later observed in the fluorescence microscope (Axioscop 2 plus, Zeiss).

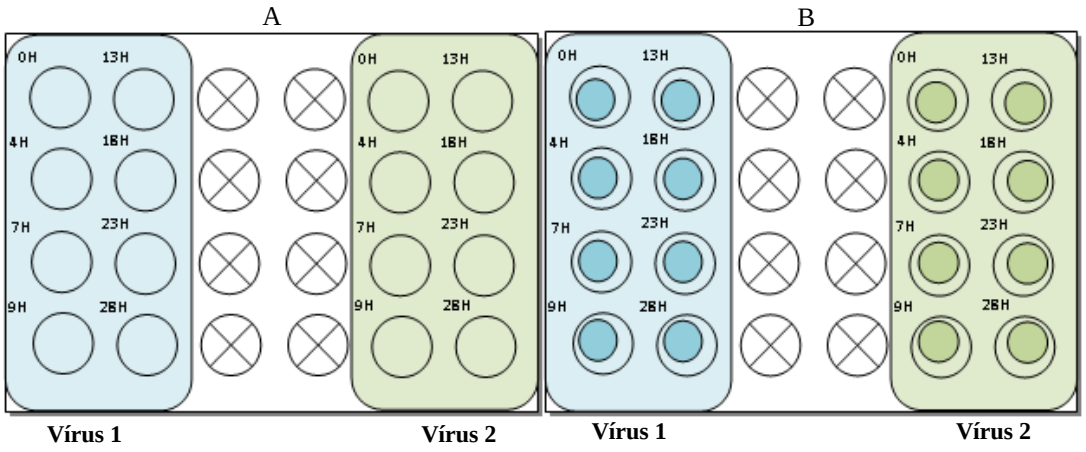

Figure 2.3: Inoculation conditions plate schemes.
[A] – kPCR plate; [B] – Monocolonal antibody staining plate.

2.4. Evaluation of HSV infection in distinct cell lines

Once optimization processes regarding inoculation conditions, time-points of infection, cell counting, and cell conditions, were established, assays were performed in order to determine the capacity of infection of the four viruses under evaluation (Table 2.1), in three distinct cell lines, in terms of progeny and infection efficiency. To do this, different multiplicities of infections (MOI) were tested (0.1, 1, 10 and 100) for each virus, to evaluate if different viral loads had any influence on the success of the infection process. To calculate the MOIs, we counted the DNA particles and not the viable viral particles *per se*, as we assumed that by the end of the viral stock preparation all viral replication and assembly had already stopped, thus giving rise to infectious viruses, once the monolayer had been completely destroyed.

For each cell line, two 24-well plates with confluent cell monolayers were prepared (as described in step 2.3.1; for further information, see Results) and inoculated with each virus at 4 different MOIs (Figure 2.4). After agitation (step 2.3.4), the inoculum was removed, the wells were washed twice with DPBS and 1 mL of fresh media was added, complemented with 4% FBS for Vero and Vero E6 cells, and 10% for the HeLa229 cell line. These steps were made in order to guarantee that all the viruses that were not able to attach/enter host cells would not affect the infection process. Infected cultures were then incubated at 37ºC with a 5% CO_2 atmosphere for 30 hours. The infectious cycle was interrupted at selected time-points (0h, 6h, 12h, 18h, 24h and 30h p.i.), where cells were harvested and stored at -20ºC until subsequent extraction and quantification. Time-point “0” refers to the time-point after agitation, following the addition of fresh medium.

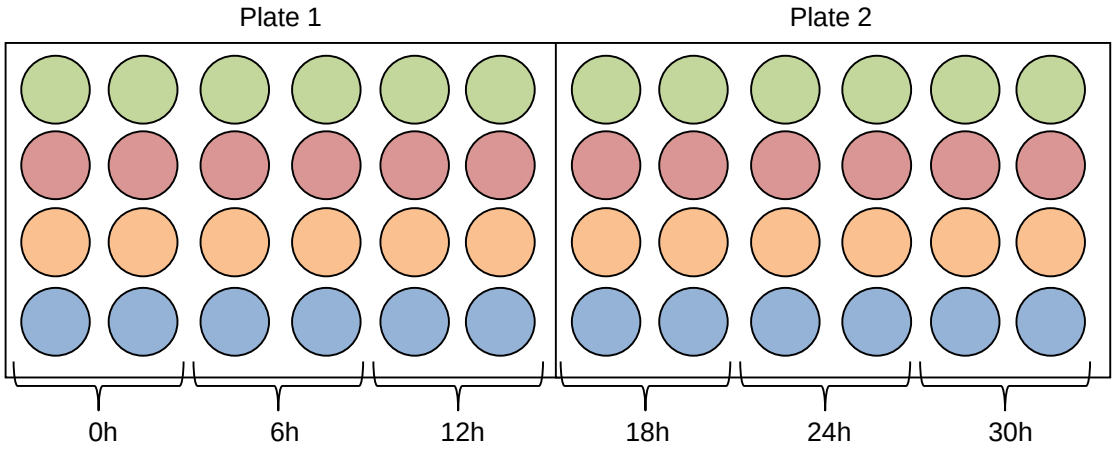

Figure 2.4: Virus inoculation plate schemes.

Two sets of plates were prepared for each virus *per* cell line. Time-points were prepared in duplicate. Each line corresponds to a different MOI: 0.1 (green), 1 (red), 10 (orange) and 100 (blue).

2.5. DNA extraction

Total DNA was extracted using the QIAamp® DNA Blood Mini Kit (Qiagen), with minor changes regarding the given protocol. Briefly, after thawing the samples harvested in step 2.4, the tubes were centrifuged at low speed, at 2500 rpm for 5 minutes, in order to isolate non-infected cells and cellular debris from viral particles. The supernatant was then collected and from this, 500 µL were added to 50 µL of Protease or Proteinase K, followed by 500 µL of buffer AL, or ATL, and agitated (Maxi Mixer Vortex 714). The samples were incubated at 56ºC for 30 minutes in a thermoblock (Thermomixer® Comfort, Eppendorf) when using AL, and 15 minutes for ATL. 500 µL of ethanol were added and the whole mixture was transferred to a mini-spin column and centrifuged (Sigma 1-14). The columns were washed with 500 µL Buffer AW1 and Buffer AW2, with spins between each treatment. Finally, the samples were eluted in 100 µL of buffer AE and stored at -20ºC until use.

2.6. Cloning

In order to develop an in-house HSV-1/HSV-2 RT-PCR system and to design a standard curve for RT-PCR experiments, a cloning assay was performed using a single copy gene from each HSV. Two genes for each HSV were chosen based of whether they were single copy genes. For HSV-1, a literature search (Szpara *et al.*, 2014) was performed to identify highly conserved genes; regarding HSV-2, both the US2 and UL27 genes were selected, as the first is the target of the standard HSV commercial kit, while the other is often used in the diagnosis and quantification of HSV DNA in the CNS (Tang et al., 1999). Primers were designed using the Primer Express® Software (Applied Biosystems) and further alignments were made using Blast (available in: http://blast.ncbi.nlm.nih.gov/Blast.cgi) to guarantee that they were HSV specific and fell in conserved gene regions. The two primers tested for both HSV are displayed in Table 2.3.

Table 2.3: Sets of primers tested.

Virus	Gene	Protein	Reference
HSV-1	UL53	Envelope glycoprotein gK	(Dolter *et al.*, 1994)
HSV-1	UL31	Nuclear protein	(Szpara *et al.*, 2014)
HSV-2	UL27	Envelope glycoprotein gB	(Tang *et al.*, 1999)
HSV-2	US2	Tegument protein	(Kang *et al.*, 2013)

Primer stock solutions were diluted to a concentration of 25 pmol/µL concentration. DNAs had already been extracted and quantified from two HSV clinical isolates (one HSV-1 and one HSV-2) from the viral stocks previously prepared (step 2.3.3). DNA serial dilutions were performed based on viral load, from a concentration of $1x10^8$ cop/µL up to $1x10^1$ cop/µL. Components for RT-PCR reactions (Table 2.4) and PCR conditions (Table 2.5) are described below:

Table 2.4: Pipetting instructions (*per* reaction).

Component	Volume (µL)
SYBR Green I	12.5
Primer F	2
Primer R	2
H_2O	3.5
Sample	5

Table 2.5: PCR cycling conditions.

Phase	Temperature	Time	Cycles
Pre-incubation	95ºC	10 min	1
Amplification	95ºC	15 sec	40
	60ºC	1 min	
Melting Curve	95ºC	15 sec	1
	60ºC	20 sec	
	95ºC	-	
Cooling	40ºC	30 sec	1

For each HSV, primer selection was based on both efficiency and slope of the obtained HSV standard curves. Primers where the respective calibration curve presented a slope of approximately - 3.3 and an efficiency of nearly 100% were chosen (Svec *et al.*, 2015).

Once chosen the fittest primers, new RT-PCR reactions were performed to amplify the two conserved gene fragments, one for each HSV, using the Thermo Scientific Phusion High-Fidelity DNA Polymerase kit (Thermo Fisher): UL31 for HSV-1 and UL27 for HSV-2. The set of primers used for this reaction (Table 2.6), components (Table 2.7) and PCR conditions (Table 2.8) are described below:

Table 2.6: Location and sequence of the primers used to amplify the desired DNA fragments.

Gene	Primer Forward	Primer Reverse	Amplicon
UL31	CTCACGCCCGCAAACAG	CGAAAAGGCCCCGATAGC	60 bp
UL27	GCGGTGGTCTTCAAGGAGAA	CACGGTCACGTCTTTGTAGTACATG	72 bp

Table 2.7: Pipetting instructions (*per* reaction).

Component	Volume (µL)
Phusion DNA Polimerase	0.5
5xPhusion HF Buffer	10
10 mM dNTPs	1
Primer F	2.5
Primer R	2.5
H2O	Up to 50 µL

Table 2.8: Real-Time PCR cycling conditions.

Phase	Temperature	Time	Cycles
Initial denaturation	98ºC	30 min	1
Denaturation	98ºC	5-10 sec	25-35
Annealing	60ºC	10-30 sec	
Extension	72ºC	15-30 sec/kb	
Final extension	72ºC	5-10 min	1

Then, the desired fragment was inserted in a linearized cloning vector (plasmid) through a ligation reaction using the CloneJET PCR cloning Kit (Thermo Fisher). A mixture was prepared with 10 µL of Reaction Buffer, 0.5 µL of the amplified PCR product (pPCR), 1 µL of pJET1.2/blunt Cloning Vector (Figure 2.5), 1 µL of T4 DNA ligase and 6.5 µL of nuclease-free Water, followed by an overnight incubation at 14ºC in a thermocycler (GeneAmp PCR System 9700, Applied Biosystems).

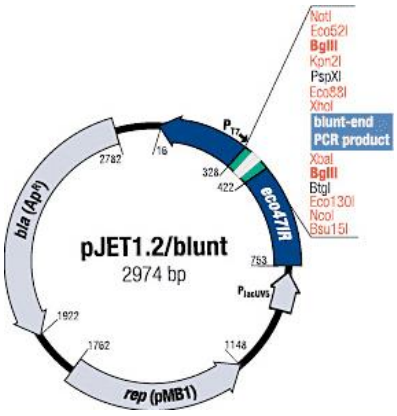

Figure 2.5: pJET1.2/blunt vector map.

For the transformation of electro-competent *E.coli* cells, 5 µL of the ligation reaction were added and the cells were left for overnight growth at 37ºC. Since only the cells with the vector have the ability to grow, all colonies were harvested and grown in LB-agar medium with ampicillin (100 µg/µL) overnight. Confirmation of transformation was achieved by Sanger sequencing.

Plasmids were purified using the PureLink™ Quick Plasmid Miniprep Kit (Invitrogen), according to the manufacturers' instructions. Briefly, the overnight LB-culture was centrifuged and the entire medium was removed. 250 µL of Ressuspension Buffer (R3) with RNase were added, followed by 250 µL of Lysis Buffer (L7) and an incubation of 5 minutes at room temperature. 350 µL of Precipitation Buffer (N4) were added, and the lysate was centrifuged for 10 minutes. The whole mixture was then transferred to a spin column and treated with 500 µL of Wash Buffer (W10 and W9), with spins between each treatment. Finally, the samples were eluted in 75 µL of TE Buffer. Plasmids were quantified by reading absorbance at 260 nm with the Qubit® and concentrations analyzed following tables 2.9 and 2.10 and equation 2.

Table 2.9: Absorbance reading and plasmid quantification.

Virus	Dilution	Concentration (ng/µL)	Concentration (g/µL)
HSV-1	1:4	7.33	7.33×10^{-9}
HSV-2	1:4	5.56	5.56×10^{-9}

Table 2.10: Determination of plasmid molecular weight.

Virus	Sequence size (bp)	Molecular Weight* (Da)	Plasmid concentration (nº plasmids/µL)
HSV-1	3034	1871796	2358285437
HSV-2	3046	1879327.02	1781653901

Note: The molecular weight of each plasmid was calculated using free software available at: http://www.currentprotocols.com/WileyCDA/CurPro3Tool/toolId-8.html. * 1 Da = 1 g/mol

$$(2)\ [Plasmid](nº\ plasmids/\mu L) = \frac{[plasmid](g/\mu L)\ x\ nº\ Avogadro\ (mol^{-1})}{Molecular\ weight\ (g/mol)}$$

In order to obtain a calibration curve, the first dilution is made at $1x10^7$ plasmids/µL, followed by serial dilutions of 1:10, up to a concentration of $1x10^0$ plasmid/µL.

2.7. Absolute Quantification assays

For extracted viral samples, RT-PCR absolute quantifications were performed, using the standard curve method, with primers regarding the UL31 gene for HSV-1 samples and the UL27 gene for HSV-2. Reactions conditions and reagents are displayed in Tables 2.4 and 2.5 above. All reactions were performed using the LightCycler®480 Real-Time PCR System (Roche, USA). For all cell lines, each 96-well plate contained the standard curve and duplicates of DNA extracted at each time-point for each MOI.

3. Results

3.1. Preliminary assays

Before evaluating the HSV infection in distinct cell lines (HeLa229, Vero and Vero E6), preliminary assays were performed to establish the optimal experimental conditions to be applied, hence ensuring that the main assays mirrored an *in vivo* HSV infection, as best as we could control.

One of the first aspects to be evaluated regarded the cellular concentration that needed to be previously added to each 24-well plates, in order to guarantee that HSV inoculation occurred on a stable 90% confluent cell monolayer able to support the entire infection cycle. For all cell lines, an optimal concentration of $3x10^5$ cells/well was found to be required to obtain a stable confluent cell monolayer, after periods of 20-24 hours for HeLa229 cells, and 30-36 hours for both the Vero and Vero E6 lines (data not shown).

Once established the ideal cellular concentration, we next determined the sufficient FBS quantity to nutritionally complement the culture medium without promoting an over-proliferation of cell cultures. Considering that both Vero and Vero E6 cells display a higher growth rate than HeLa229 cells, and have tendency to vertically overlap, smaller quantities of FBS had to be added to the culture medium to obtain stable confluent monolayers at the time of the experiments. Whereas for HeLa229 cells, 10% of FBS was used, for both Vero and Vero E6 cells, 4% was found to be sufficient (data not shown).

We then sought to evaluate the ideal inoculation *modus operandi* (centrifugation *vs.* agitation), so that the success of the inoculation process was guaranteed, while maintaining it as less artificial and stressful as possible for mimicking an *in vivo* infection. For higher robustness, two HSV-2 clinical isolates, differing ~2.5-times in viral load (which corresponds to MOIs of ~40 [Sample 1] and ~100 [Sample 2]), were used. Regardless the inoculation *modus operandi* tested, the two HSV-2 isolates seem to exhibit a similar infectious/life cycle pattern of ~23 hours, time where viral progeny peaks for both isolates, apparently stabilizing after that (Figure 3.1). In addition, the HSV infection does not seem to be influenced by viral load when centrifugation is performed (Figure 3.1A), contrarily to that observed with agitation, where differences ranging from 2.2- to 5.3-fold were detected throughout the infectious cycle among the two HSV-2 clinical isolates (Figure 3.1B). These findings were also supported by comparing each infection between the two inoculation processes (Figure 3.2). Although no differences were seen until 9 hours p.i. for both HSV-2 isolates, a different scenario was observed after this time-point for the virus with the lowest load (Figure 3.2A). Significant discrepancies were seen in this case, where 3-fold higher progenies were obtained, in average, for centrifugation when compared with agitation. This was not surprising, as centrifugation mechanically forces viral attachment to the host cells, and at 4ºC no cellular metabolism occurs, avoiding any viral entry. The entry process is hence synchronized, ensuring that, at higher temperatures, some of attached virus will later enter at the same rate. In opposition, agitation at 37ºC allowed both the viral attachment and entry into the host cells at different rates. On the other hand, when HSV-2 viral load is higher, infection efficiency seems to be similar among the two inoculation processes (Figure 3.2B), as progenies generated throughout the cycle were analogous, suggesting that viral load may be a critical factor for the success of the HSV-2 infection, at least for the tested Vero cell line. These preliminary RT-PCR absolute quantification results were

further supported by immunofluorescence assays (performed in parallel), where Vero cell alterations could be seen as HSV-2 infection progressed, being slower with agitation (Figure 3.3) and lower viral loads (data not shown).

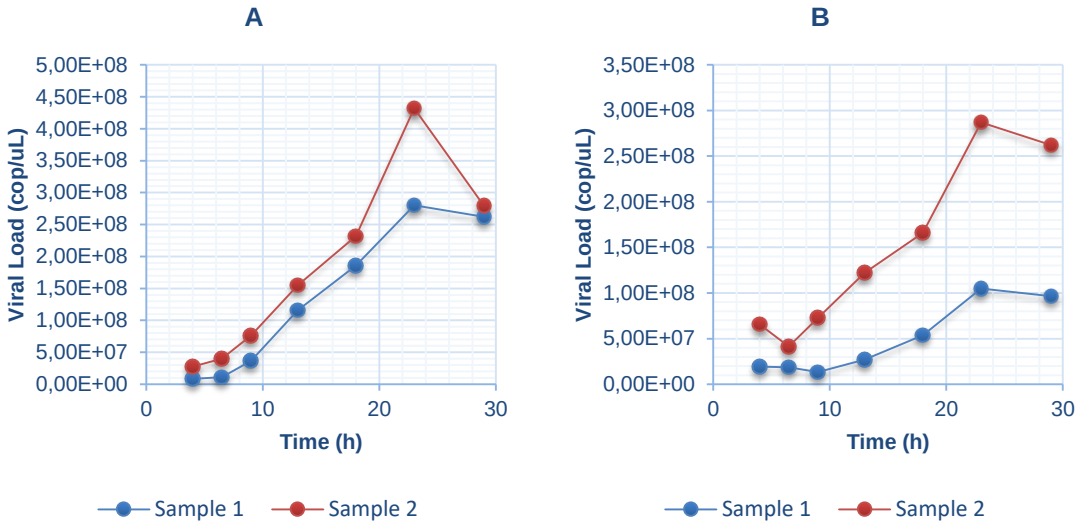

Figure 3.1: Growth curves of two HSV-2 clinical isolates with different viral loads.

[A] – Centrifugation; **[B] -** Agitation

Confluent cell monolayers were infected with two viral samples and incubated for 29 hours at 37ºC and a 5% CO_2 atmosphere. Cells were harvested at different time points in order to assess progeny and compare the two processes.

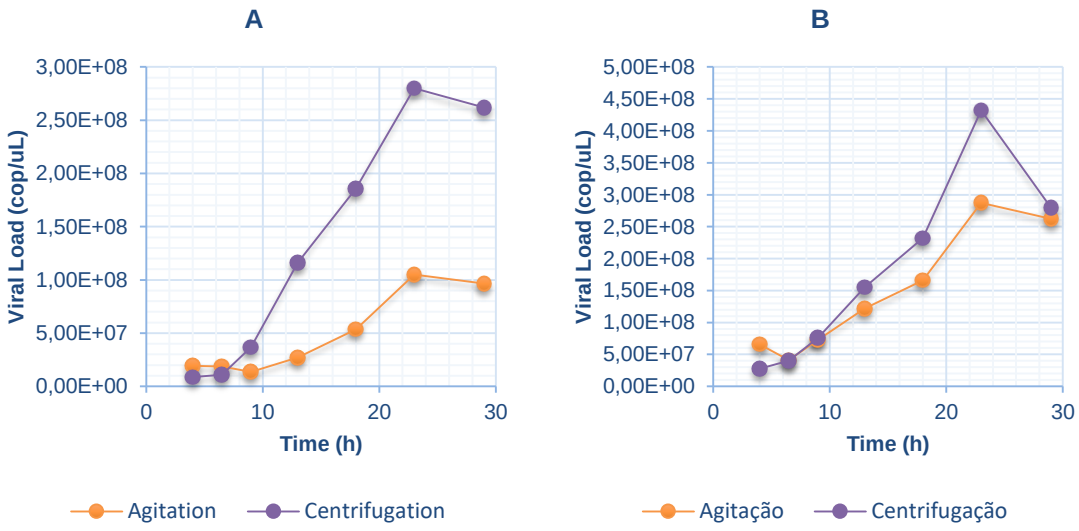

Figure 3.2: Growth curves of two HSV-2 samples with different viral loads.

[A] – Sample 1; **[B] –** Sample 2.

Confluent cell monolayers were infected with two HSV-2 samples and incubated for 29 hours at 37ºC and a 5% CO_2 atmosphere. Cells were harvested at different time points in order to assess progeny and compare the two processes.

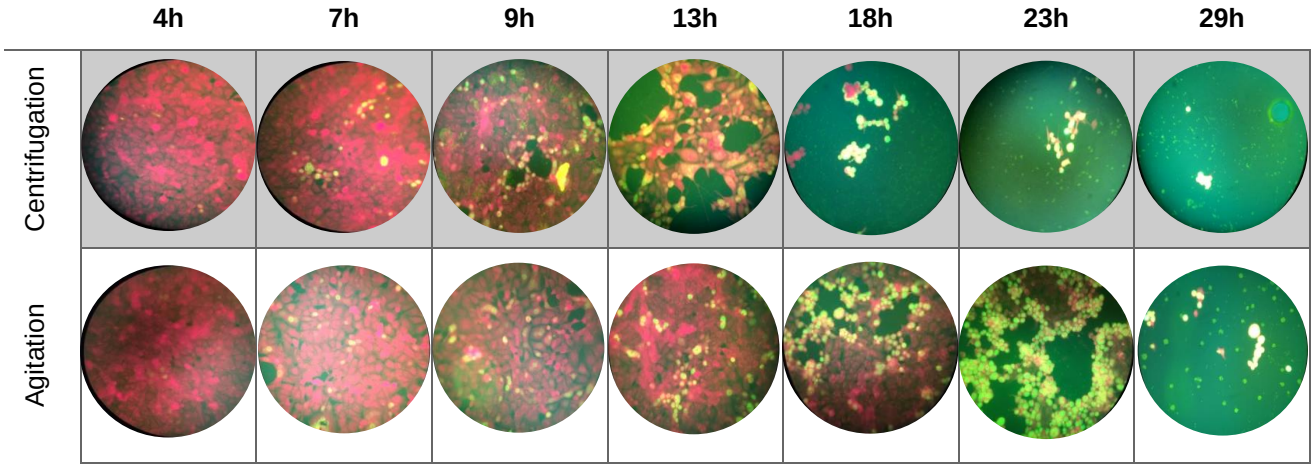

Figure 3.3: Evolution of a HSV infection over time, in a monoclonal antibody staining assay. Cells were stained with monoclonal antibodies at the indicated time-points of infection. Uninfected cells are stained in red, and infected cells can be seen as fluorescent green. Over time, the number of cells diminishes, and in the end, there are almost no cells left, as a HSV infection lead to cell lysis.

3.2. Evaluation of HSV infections in distinct cell lines

Considering the preliminary results for the HSV-2 subtype in Vero cell line, likely pointing viral load as an important player in the efficiency of the infection, further studies were conducted using two other HSV-2 (C and D) and two HSV-1 (A and B) clinical isolates at four different MOIs (0.1, 1, 10 and 100), as well as two additional cell lines (HeLa229 and Vero E6) exhibiting different phenotypic and molecular features. We can assume that similar initial concentrations of each virus were added to all plates for a specific MOI and for each cell line.

In order to assess if both capacity and efficiency of HSV infection depend on the HSV subtype/strain and/or on the infected cell line, RT-PCR absolute quantifications were performed throughout multiple time points of infection (0h, 6h, 12h, 18h, 24h and 30h) in each cell line. Based on both slopes and efficiencies of calibration curves (see “Material and Methods” for details), primers regarding the UL27 and UL31 genes were selected for RT-PCR absolute quantification of HSV-2 and HSV-1 strains, respectively.

Unpredictably, contrarily to preliminary assays, the HSV life cycle was longer, and at 30 hours p.i. there was not a viral load stabilization, indicating that DNA continued to be synthesized for all viral isolates, in the three cell lines (including the previously tested Vero cell line).

3.2.1. HSV-2 infections

Unexpectedly, for the three cell lines (including the previously tested Vero cell line), the life cycle observed for the two HSV-2 clinical isolates (C and D) was longer than that found in the preliminary assays. Indeed, no viral load stabilization was seen at 30 hours p.i., indicating that DNA continued to be synthesized for all viral strains. Considering that clinical isolate C was used in the preliminary assays at MOI of 100 (isolate 2), we would expect that, at least for this virus, the infectious process would have had, approximately, the same duration. However, this was not observed. The reason for this may be

due to viral stock preparation before the experiments, where the virus was subjected to multiple rounds of freezing/thawing, likely impacting both the infectiousness and rate of viral infection, when inoculations were performed using a viral aliquot immediately after thawing. In opposition, in the preliminary assays, this isolate was directly used without any step of freezing/thawing.

For clinical isolate D, regardless the cell line used, continuous microscopic observation for each MOI revealed no significant CPE during the period under evaluation. Curiously, no viral particles were apparently quantified by RT-PCR assays (data not shown). Considering that standard curves (present in the same plate as extracted DNA samples at each time-point for each MOI and for each cell line) were generated, one can discard the occurrence of any problem in the RT-PCR reactions or selected primers. The only plausible explanation points to a failure in the infection process (possibly due to virus viability loss). As all the inoculum was removed in each condition, no viral particles remained in the culture to be later extracted and detected by RT-PCR assays. For this reason, this clinical isolate was discarded from this study.

On the other hand, for clinical isolate C, evident CPE could be observed microscopically from MOI of 1, where damages were visible at 30 hours p.i. for all cell lines (Figure 3.4), to MOIs of 10 and 100, where the monolayer of all three cell lines had been practically destroyed after 12-18 hours of infection.

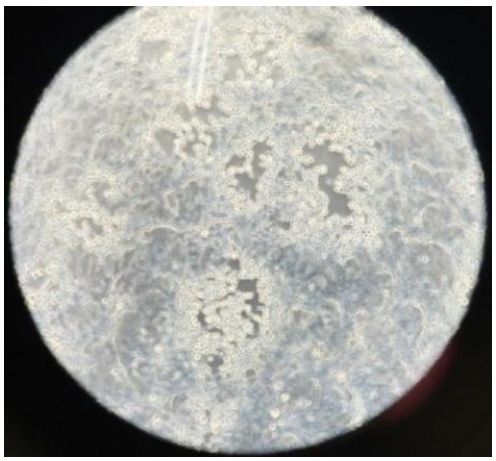

Figure 3.4: HSV-2 isolate C infection *in vitro*, at a MOI of 1, 30 hours p.i.

Regarding HSV-2 isolate C, at 0h p.i. (Figure 3.5), time period when host cell attachment is thought to occur, the Vero E6 cell line always presented the lowest viral concentrations, regardless the MOI, while similar attachment rates were seen in both HeLa229 and Vero cells, with the exception of MOI of 0.1. Moreover, DNA appears to have always been synthesized earlier (mostly at 6h p.i.) in the Vero E6 cell line for all MOIs (Figure 3.6), with a lag of ~6h (at least) when compared to both HeLa229 and Vero cells. The only exception occurred for MOI of 1, where this isolate displayed similar behavior in both HeLa229 and Vero E6 cells. Curiously, despite the disparities in the observed attachment capacities, the generated DNA particles at 30h p.i. were identical for each MOI and in each cell line (Figure 3.5).

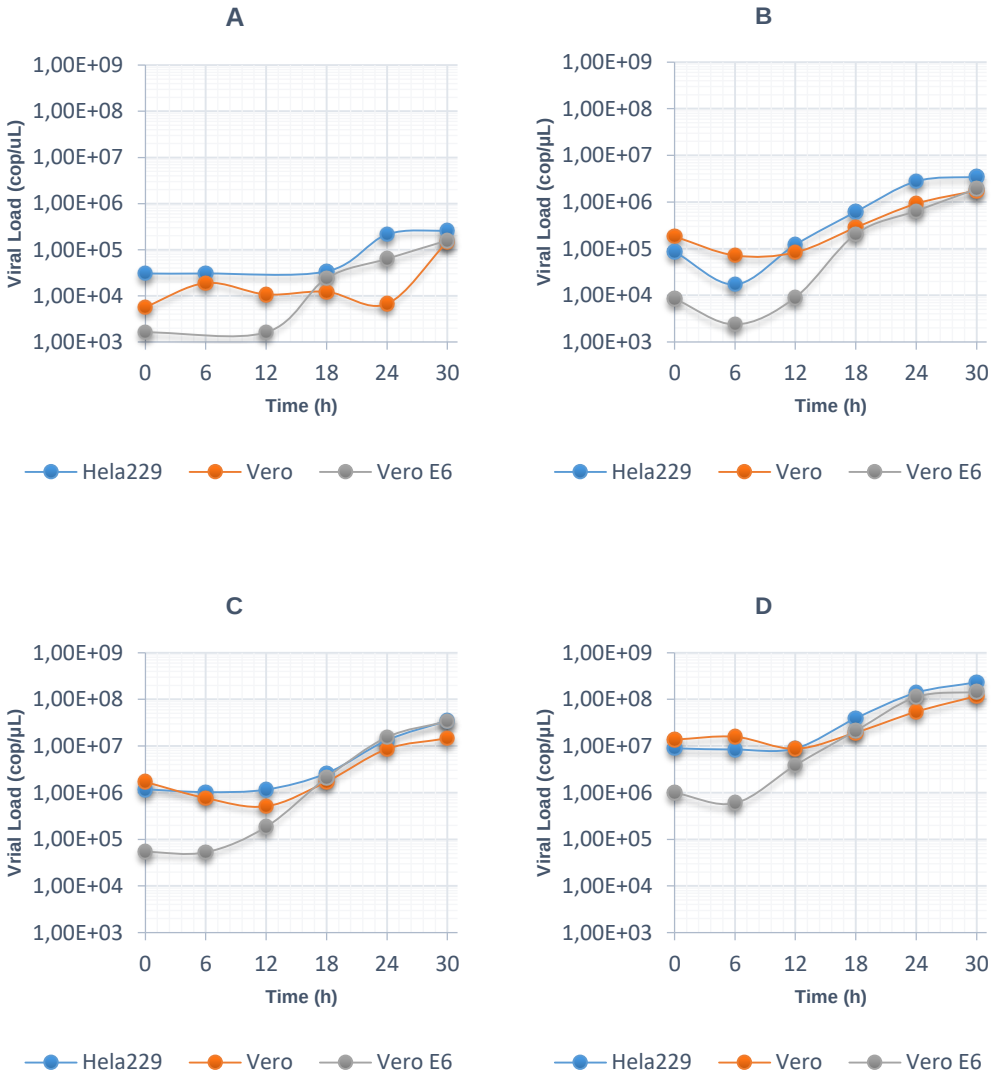

Figure 3.5: HSV-2 isolate C growth curves in HeLa229, Vero and Vero E6 cells at four MOIs.
[A] – MOI 0.1; **[B] –** MOI 1; **[C] –** MOI 10; **[D]** – MOI 100.
Confluent cell monolayers were infected with the indicated virus at four distinct MOIs in HeLa 299 (blue), Vero (orange) and Vero E6 (grey) cells. Viral load values are expressed on a logarithmic scale.

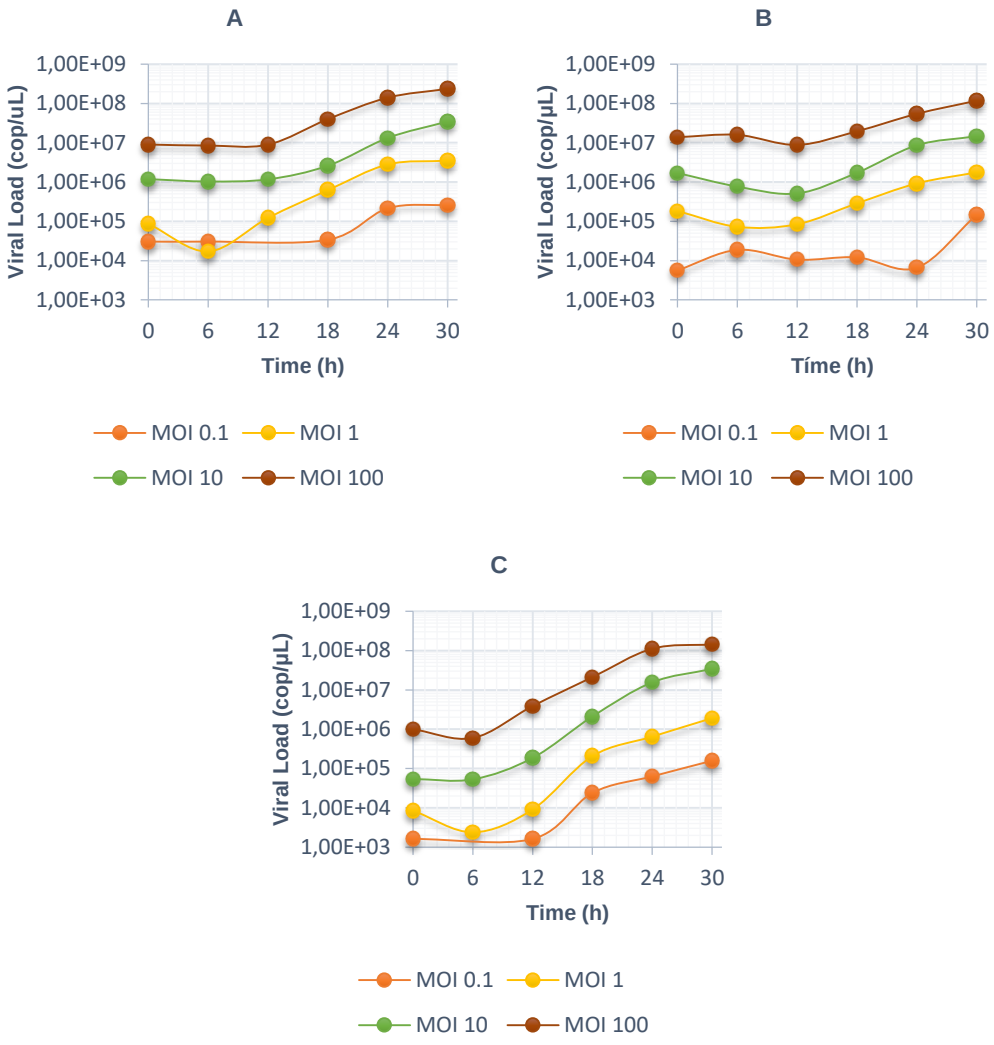

Figure 3.6: HSV-2 isolate C growth curves in distinct cell lines, at four different MOIs.

[A] – HeLa229 line; **[B] –** Vero line; **[C] –** Vero E6 line.

Results were analyzed in terms of MOI, in each cell line. MOIs of 0.1 (orange), 1 (yellow), 10 (green) and 100 (red) were compared between to two samples. Viral load values are expressed on a logarithmic scale.

3.2.2. HSV-1 infections

For both clinical isolates (A and B), HSV-1 life cycle did not seem to end at 30h p.i. for all cell lines regardless MOI, as no viral stabilization was achieved until this time-point, as seen for HSV-2 clinical isolate C.

Little cellular destruction was microscopically observed for both HSV-1 clinical isolates at MOIs of 0.1 and 1 (Figure 3.7), even at 30h p.i.. On the other hand, for MOIs of 10 and 100, cellular damages were observed as soon as 6/12 hours p.i. for all cell lines, with total CPE visible at 30h p.i.. These phenomena were more evident in both HeLa229 and Vero E6 cells than in the Vero cell line.

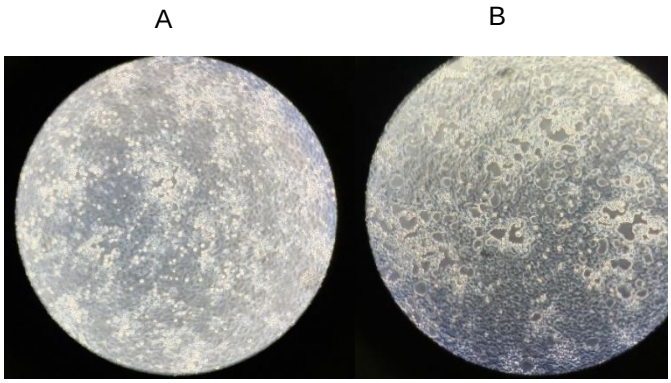

Figure 3.7: HSV-1 infection *in vitro.*

[A] – HSV-1 infection (isolate A) in Vero cells, at a MOI of 1, 30 hours p.i.

[B] – HSV-1 infection (isolate A) in Vero E6 cells, at a MOI of 1, 30 hours p.i.

At a MOI of 0.1 (Figure 3.8), both HSV-1 clinical isolates (A and B) seemed to have lower attachment affinities towards HeLa229 cells when comparing to the remaining cell lines. DNA started to be synthesized at 12h p.i., except for clinical isolate A, where synthesis in Vero cells began earlier, 6h p.i.. At 30h p.i., similar DNA particles had been originated for almost all cell lines, although higher viral loads were found for clinical isolate A in HeLa229 cells.

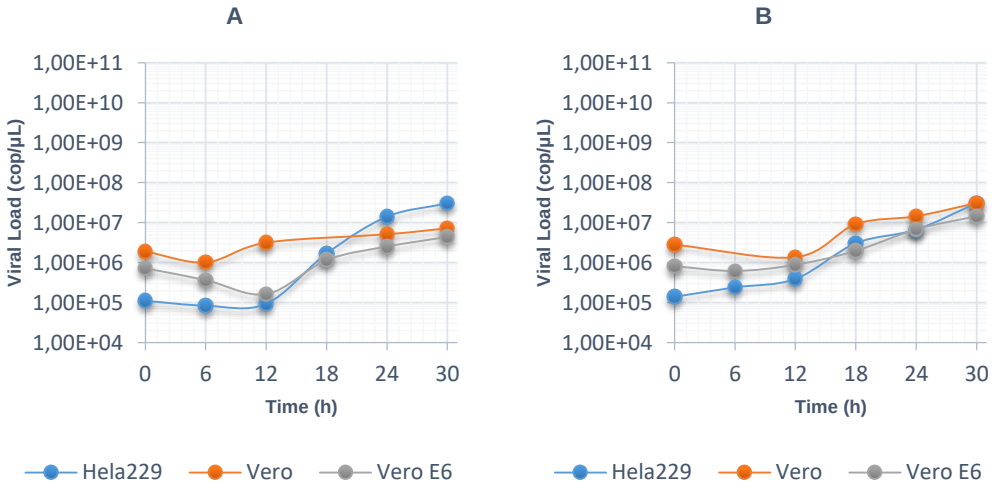

Figure 3.8: Clinical isolates A and B growth curves in the three cell lines, at a MOI of 0.1.

[A] – Clinical isolate A; **[B] –** Clinical isolate B.

Confluent cell monolayers were infected with the indicated virus at a MOI of 0.1 in HeLa 299 (blue), Vero (orange) and Vero E6 (grey) cells. Viral load values are expressed on a logarithmic scale.

On the other hand, a slightly different attachment scenario was seen for MOIs of 1, 10 and to a lesser extent 100 (Figure 3.9), where both HSV-1 clinical isolates exhibited lower attachment affinities towards Vero E6 cells comparing to the remaining cell lines. For both clinical isolates, DNA generation appears to begin at 6h p.i. for both HeLa229 and Vero E6 cells regardless MOI, whereas a delay of ~6h was seen for Vero cell line (Figure 3.10). At 30h p.i., clinical isolate B seemed to generate similar DNA molecules regardless cell line, while higher viral loads of clinical isolate A were always found for HeLa229 cells (Figure 3.9).

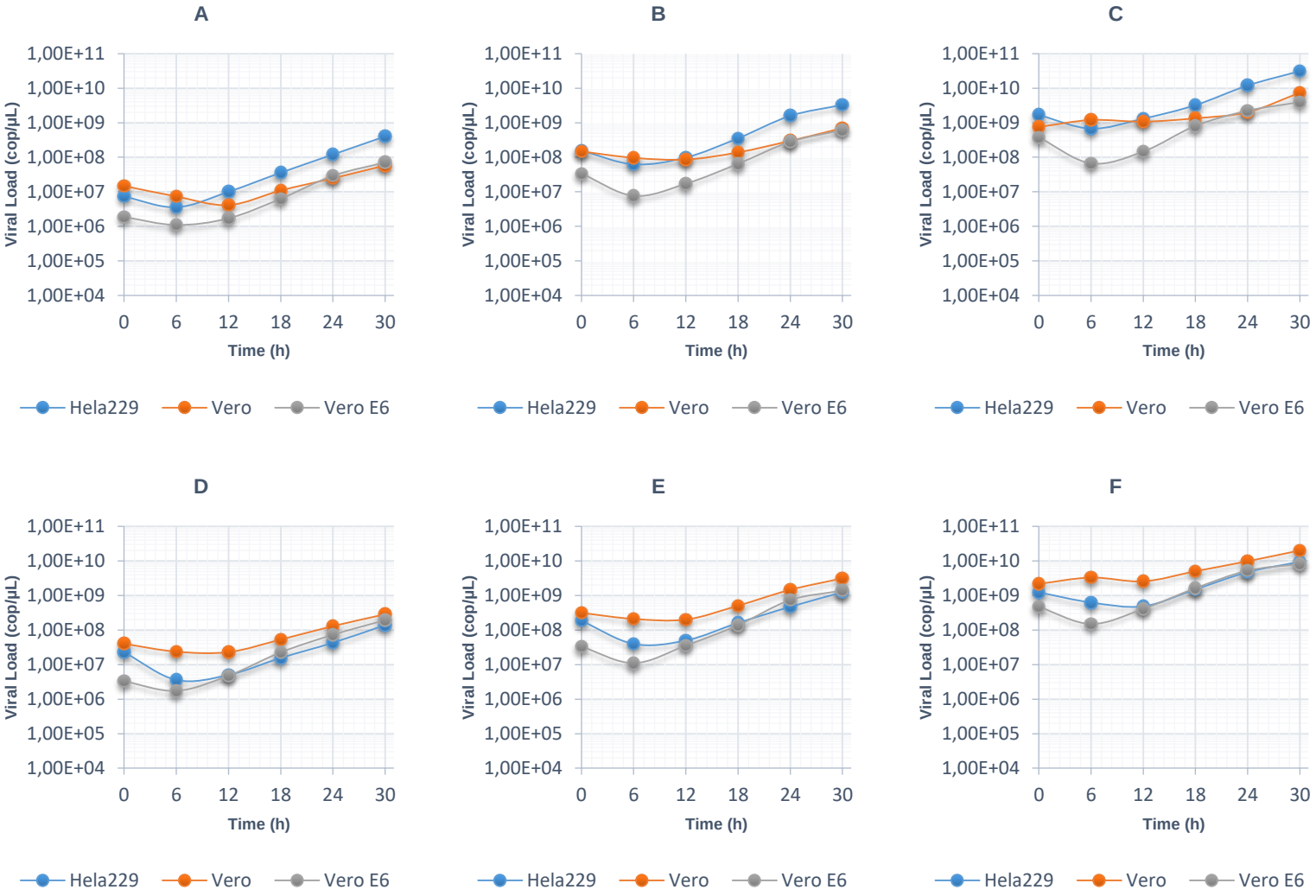

Figure 3.9: HSV-1 isolates A and B growth curves in the three cell lines, at MOIs of 1, 10 and 100.

[A] –Clinical isolate A, MOI 1; **[B] -** Clinical isolate A, MOI 10; **[C] –** Clinical isolate A, MOI 100;

[D] - Clinical isolate B, MOI 1; **[E] –** Clinical isolate B, MOI 10; **[F] –** Clinical isolate B, MOI 100.

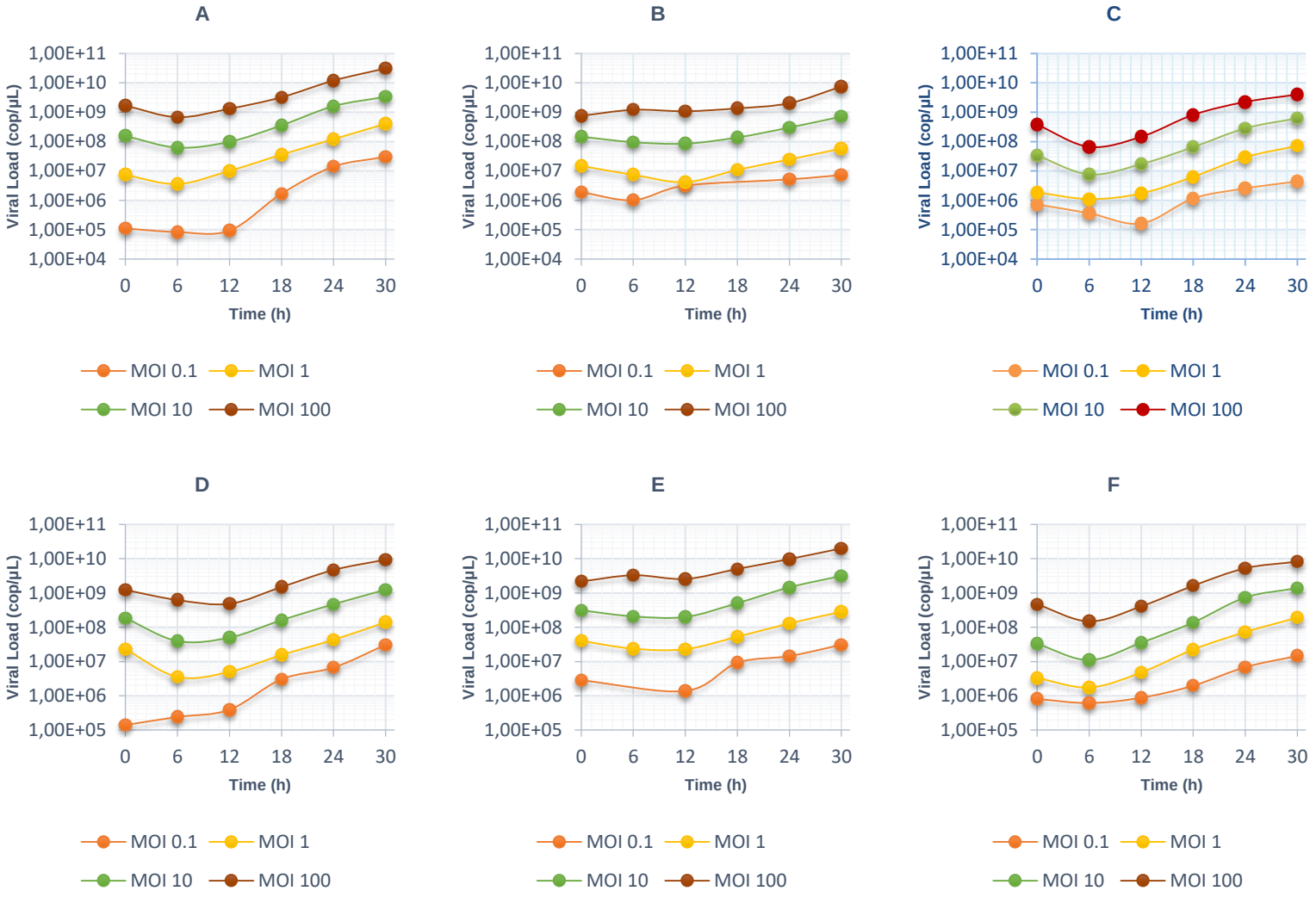

Figure 3.10: HSV-1 isolates A and B growth curves in the three cell lines, at four different MOIs.

[A] – HeLa229**,** Clinical isolate A; **[B] -** Vero, Clinical isolate A; **[C] –** Vero E6, Clinical isolate A;

[D] - HeLa229, Clinical isolate B; **[E] –** Vero, Clinical isolate B; **[F] –** Vero E6, Clinical isolate B.

3.3. Evaluation of HSV infection yields in distinct cell lines

In order to assess infection efficiency, virus yields were calculated based on the initial and final viral loads for each sample. For clinical isolate C, the Vero E6 cell line seemed to be the most appropriated one for HSV-2 growth, always exhibiting efficiency rates considerably higher for all MOIs, including a remarkable value of ~626 for MOI 10 (Table 3.1; Figure 3.11). In fact, for this MOI, yield values regarding viral growth in the Vero E6 cell line were 20 and 70 times higher when compared to those of HeLa229 and Vero cells, respectively.

For both HSV-1 clinical isolates, higher infection efficiencies were clearly obtained in HeLa229 cells, with higher values (~270 and 219 for isolate A and B, respectively) at MOI 0.1. Curiously, for increasing MOIs, lower efficiency rates were observed in this cell line.

Overall, worst viral infection yields were always observed for the Vero cell line regardless MOI, with values ranging from ~ 4 to 26.

Table 3.1: Viral yield values for each sample, in three distinct cell lines and four MOIs.

Sample		*Cell Line*	*MOI 0.1*	*MOI 1*	*MOI 10*	*MOI 100*
HSV-1	*Sample A*	HeLa229	276,36	55,15	21,45	18,37
		Vero	3,79	3,91	4,80	9,83
		Vero E6	6,09	38,13	18,36	10,48
HSV-1	*Sample B*	HeLa229	219,71	6,08	6,74	7,67
		Vero	10,94	7,11	10,04	9,23
		Vero E6	17,95	58,63	42,55	17,52
HSV-2	*Sample C*	HeLa229	8,56	40,35	29,57	25,98
		Vero	25,93	9,58	8,63	8,59
		Vero E6	97,18	224,29	626,20	143,51

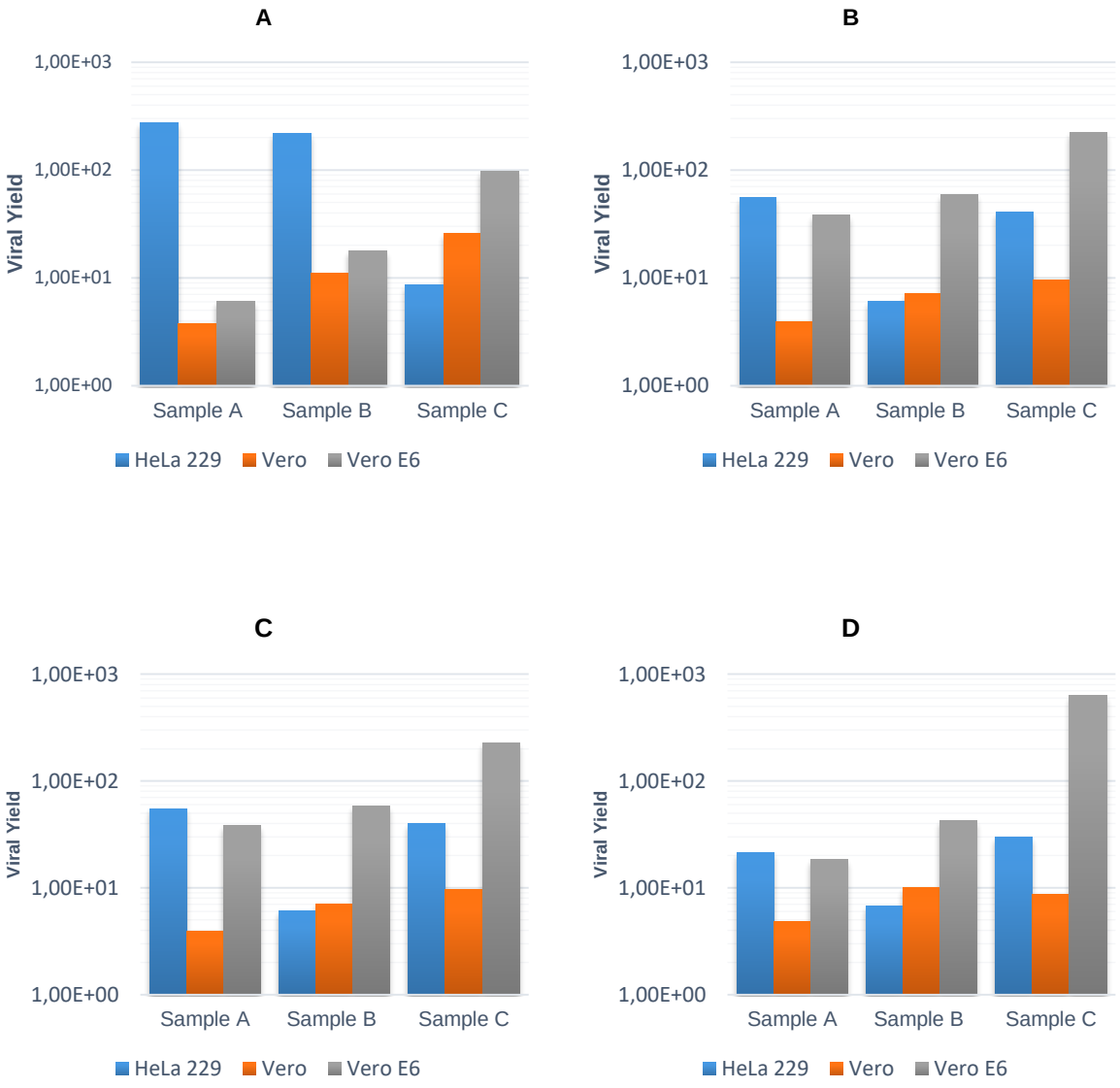

Figure 3.11: Viral yield at four MOIs.

[A] – MOI 0.1; **[B] –** MOI 1; **[C] –** MOI 10 **[D] –** MOI 100.

Yield values were evaluated in HeLa229 (blue), Vero (orange) and Vero E6 (grey) cells, for the four MOIs. Values are expressed on a logarithmic scale.

4. Discussion

Genital herpes is currently one of the most prevalent STIs worldwide (Smith *et al.*, 2002). However, despite the fruitful research performed in the later years, we are still far from understanding the molecular features underlying HSV genital infections, as viral cellular tropism appears to be not as restrictive as traditionally assumed. Indeed, there has been an increase in the number of primary genital infections caused by HSV-1 (usually associated with oro-facial lesions), even though HSV-2 still remains the most prevalent subtype found in genital herpetic lesions. Therefore, in order to contribute for the understanding of the pathogenesis of human herpes genital infections, the current MSc thesis intends to evaluate whether HSV subtype/strain and/or infected tissue impacts both capacity and efficiency of viral infection, in terms of replication rate and progeny.

Concerning the HSV life cycle, no consensual literature was found, as some authors claim that HSV is able to infect and lyse host cells within 15 hours (Jenkins *et al.*, 1996, Lehman *et al.*, 1999, Tang *et al.*, 1999), while others reported processes of ~24 hours (Roizman *et al.*, 2003, Schiffer *et al.*, 2013). Our preliminary assays corroborate the later, as infection cycles of ~23 hours were obtained. However, in our main assays, longer infectious cycles were seen (~30h), which could be explained by the multiple rounds of freezing/thawing in the viral stock preparation, likely impacting both the infectiousness and rate of viral infection (GREIFF *et al.*, 1954, Pinsky *et al.*, 2003, Hansen *et al.*, 2005)

For all HSV-1 and HSV-2 clinical isolates, similar infection patterns were observed for every MOI except 0.1, regardless cell line. Despite dissimilar viral loads seen at 0h p.i., the observed consecutive 10x load increments for higher MOIs (Tables A2-4 from Appendix 2) suggest that initial viral concentrations do not appear to affect adherence to host cells. Nevertheless, for a MOI of 0.1, HSV-2 attachment efficiency was 70x lower than that observed for both HSV-1 isolates, with a difference ~140x lower at the highest MOI of 100. Corroborating this, Trybala *et al.* (Trybala *et al.*, 2000) showed that both HSVs display different affinities towards the HS molecule, is essential for the viruses initial binding. These differences were also seen by Vahlne *et al.* (Vahlne *et al.*, 1980), who demonstrated that HSV-1 virions were more easily adsorbed that those of HSV-2 for a specific cell type.

We do not know whether attached viruses are able to effectively enter into host cells, neither if the host cell is permissive to the infection of more than one virus. As a HSV infection causes multiple alterations in the cell surface, such as membrane modifications and loss of matrix binding proteins (Blaho *et al.*, 2005), it is possible that more than one virus infects a single cell, by taking advantage of the cell's deterioration. At a MOI of 0.1, where we have 10 cells for each virus, we can assume that almost every virus was able to entry into a host cell and originate high progeny. This assumption was not so intuitive for higher MOIs, since we don't know whether one viral particle gives rise to 1 or 100 progeny virions.

For all HSV-1 and HSV-2 clinical isolates, DNA started to be synthesized nearly 6-12h p.i., increasing throughout the cycle until it peaked, stabilizing or decelerating after that due to a higher viral assembly and release (Figure 3.6; 3.10). Curiously, until DNA synthesis began, viral concentrations were found to first decrease during a ~6h-period in almost all assays, regardless the MOI and cell line. Similar behaviors had been already reported in the literature (Nicola *et al.*, 2004), where this apparent

temporary decrease was presumed to represent virion gradual degradation and not penetration into the cytosol. During this ~6h time-period, we believe that HSV replication starts to take place, often with simultaneous generation of infectious progeny virus. To support this, replication periods between 3-6h p.i. and 12-18h p.i. have been reported in the literature (Blaho *et al.*, 2005, Ikeda *et al.*, 2011). On the other hand, monolayer destruction seems to be phenotypically different between HeLa229 and both Vero and Vero E6 cells, with CPE in the later being characterized by a random cell concentration in the monolayer that continuously spreads until total cell lysis (Figure 3.4), while CPE in HeLa229 cells appears to have a uniform cellular infection distribution in the monolayer that ends up with cell lysis. Considering that HeLa229 is a human epithelial cell line isolated from a cervix adenocarcinoma whilst Vero/Vero E6 cells are isolated from kidney cells extracted from an African green monkey, we can speculate whether the last are a good *in vitro* model to mimic genital infections *in vivo*.

Regarding viral infection capacity in all three host cell lines, Vero E6 cells seem to be unquestionably the most appropriated ones for HSV-2 growth, always exhibiting efficiency rates considerably higher for all MOIs, where differences of up to 6-fold were seen for MOI 10 when compared with the lowest value given by MOI 0.1 (~626 *versus* ~97) (Table 3.1; Figure 3.11). On the other hand, HeLa229 cells appeared to be the most suitable for HSV-1 infection at the lowest MOI, indicating that the replication success is higher for smaller inoculums. This yield decreases with the increase of the MOIs (Table 3.1; Figure 3.11). There seems to be some kind of inhibitory process that does not allow the viruses to replicate at such a higher pace as that for smaller MOIs (Figures 3.6; 3.10; 3.11). One option is the fact that a lot of viruses appear to attach to the cell's surface, but only a small percentage have the ability to penetrate it and initiate the replication cycle. On the other hand, it is possible that the same number of viruses enter a host cell, but replication rates suffer some kind of inhibition/saturation, making the process not as efficient. Nevertheless, as mentioned before, it does not seem that an increase in the inoculum poses as an inhibition to virus attachment, since all attached cells can be accounted for. Overall, in the described conditions, the Vero cell line had the worst viral growth results regardless MOI, displaying the lowest replication rate yields (Table 3.1; Figures 3.11). This does not coincide with the literature, where viral yields were shown to be similar in both Vero and HeLa229 cells (Nicola *et al.*, 2003). It was also demonstrated that HSV-1 grew to between 2 and 5 times higher titers in Vero cells when compared with HeLa229 cells, suggesting a faster viral growth (Nguyen *et al.*, 2005). The most plausible explanation for the occurred relies on the fact that high-passage Vero cell flasks are commercially purchased, so that no more than 4-5 passages are made, before losing cell properties. This parallels a previous study performed for another cell line (Hampar *et al.*, 1965), where it was stated that, beyond 10 passages, the time required for complete HSV cell destruction after a viral infection increased. On the other hand, a decrease in productive viral replication can occur when cells are left more than a day after reaching confluency prior to an infection. It was seen that, when Vero cells reached 100% confluency and were not passed or infected, they would vertically overlap and/or die (Ammerman *et al.*, 2008).

Although there are multiple studies that intended to evaluate putative differences in HSV subtypes infectivity, none of them is conclusive, being sometimes contradictory. For instance, while some authors argue that HSV-1 generally grows to a higher pace than HSV-2 (Docherty *et al.*, 1971), others state that

HSV-2 strains generally show faster and more complete shut off of host protein synthesis than HSV-1 strains (Aguilar *et al.*, 2006). Regardless MOI and host cell line, our results showed that HSV-2 always exhibits lower attachment capacities than HSV-1, apparently growing at a slower pace throughout the infection cycle (Figures 3.5; 3.8; 3.9). However, concerning viral DNA synthesis, discrepancies among HSV subtypes were only seen between cell lines. Indeed, for instance, HSV-2 seemed to always yield more progeny virions than both HSV-1 clinical isolates in Vero E6 cells (Table 3.1; Figure 3.11). Although we cannot state that this higher HSV-2 infection success might occur *in vivo*, it is not nonsense to speculate that, in genitalia, HSV-2 may have acquired evolutionary strategies allowing a better host immune evasion than for the recently emerging HSV-1 genital herpes, which may be not yet adapted to this biological niche. Nevertheless, for both HSV subtypes in general, progeny appears to have been generated earlier (mostly at 6h p.i.) in the Vero E6 cell line for all MOIs, while for the remaining cells (HeLa229 and Vero) progenies were mostly seen with a lag of ~6h (at least) (Figures 3.6; 3.10).

In the future, biological replicas should be made, in order to further confirm the obtained results. To do this, all the assays should be repeated, using a different aliquot from the viral stocks produced. In addition, other cells lines could be studied, namely MRC-5. This is a fibroblastic cell line, often used in HSV studies, commonly used for shell vial tests, for HSV detection; however, it is frequently used for CMV in INSA, but not for HSV, hence not being used as an additional tested cell line.

We also intend to study *in vitro* selective pressure. As mentioned before, it is possible that multiple passages in the Vero cell line *in vitro* can affect their viability, one possible reason for the results obtained. Genomic studies should also be made of both HSV sub-types, to determine if the viruses developed some kind of resistance to growth on Vero cells.

Viral stocks were only prepared in the Vero cell line. This was due to the fact that Vero cell line is the preferential line for HSV studies. Nevertheless, it is not known whether viral propagation in different cell lines would lead to differences in infections capacities in the respective cell line. So, we also intend to produce viral stocks Vero E6 and HeLa229 cells.

Finally, one additional study should be made regarding freezing and de-freezing viral stocks, in order to evaluate if there is any loss of infection capacity.

5. References

Aguilar, J.S., Devi-Rao, G.V., Rice, M.K., Sunabe, J., Ghazal, P. and Wagner, E.K. (2006). Quantitative comparison of the HSV-1 and HSV-2 transcriptomes using DNA microarray analysis. *Virology* **348,** 233-241.

Ammerman, N.C., Beier-Sexton, M. and Azad, A.F. (2008). Growth and maintenance of Vero cell lines. *Curr Protoc Microbiol* **Appendix 4,** Appendix 4E.

Bacon, T.H., Levin, M.J., Leary, J.J., Sarisky, R.T. and Sutton, D. (2003). Herpes simplex virus resistance to acyclovir and penciclovir after two decades of antiviral therapy. *Clin Microbiol Rev* **16,** 114-128.

Baines, J.D. (2011). Herpes simplex virus capsid assembly and DNA packaging: a present and future antiviral drug target. *Trends Microbiol* **19,** 606-613.

Beauman, J.G. (2005). Genital herpes: a review. *Am Fam Physician* **72,** 1527-1534.

Bittencourt, M.e.J., Freitas, L.K., Drago, M.G., Carvalho, A.H. and Nascimento, B.A. (2016). Cutaneous neonatal herpes simplex virus infection type 2: a case report. *An Bras Dermatol* **91,** 216-218.

Blaho, J.A., Morton, E.R. and Yedowitz, J.C. (2005). Herpes simplex virus: propagation, quantification, and storage. *Curr Protoc Microbiol* **Chapter 14,** Unit 14E.11.

Boehmer, P.E. and Nimonkar, A.V. (2003). Herpes virus replication. *IUBMB Life* **55,** 13-22.

Bowman, B.R., Baker, M.L., Rixon, F.J., Chiu, W. and Quiocho, F.A. (2003). Structure of the herpesvirus major capsid protein. *EMBO J* **22,** 757-765.

Brown, J.C. and Newcomb, W.W. (2011). Herpesvirus capsid assembly: insights from structural analysis. *Curr Opin Virol* **1,** 142-149.

Bucks, M.A., O'Regan, K.J., Murphy, M.A., Wills, J.W. and Courtney, R.J. (2007). Herpes simplex virus type 1 tegument proteins VP1/2 and UL37 are associated with intranuclear capsids. *Virology* **361,** 316-324.

Campadelli-Fiume, G., Menotti, L., Avitabile, E. and Gianni, T. (2012). Viral and cellular contributions to herpes simplex virus entry into the cell. *Curr Opin Virol* **2,** 28-36.

Chilukuri, S. and Rosen, T. (2003). Management of acyclovir-resistant herpes simplex virus. *Dermatol Clin* **21,** 311-320.

Connolly, S.A., Jackson, J.O., Jardetzky, T.S. and Longnecker, R. (2011). Fusing structure and function: a structural view of the herpesvirus entry machinery. *Nat Rev Microbiol* **9,** 369-381.

Crumpacker, C.S. and Schaffer, P.A. (2002). New anti-HSV therapeutics target the helicase-primase complex. *Nat Med* **8,** 327-328.

de Silva, S. and Bowers, W.J. (2009). Herpes Virus Amplicon Vectors. *Viruses* **1,** 594-629.

Docherty, J.J., O'Neill, F.J. and Rapp, F. (1971). Differential susceptibility to herpes simplex viruses of hamster cell lines established after exposure to chemically inactivated herpesvirus. *J Gen Virol* **13,** 377-384.

Dolan, A., Jamieson, F.E., Cunningham, C., Barnett, B.C. and McGeoch, D.J. (1998). The genome sequence of herpes simplex virus type 2. *J Virol* **72,** 2010-2021.

Dolter, K.E., Ramaswamy, R. and Holland, T.C. (1994). Syncytial mutations in the herpes simplex virus type 1 gK (UL53) gene occur in two distinct domains. *J Virol* **68,** 8277-8281.

Döhner, K., Wolfstein, A., Prank, U., Echeverri, C., Dujardin, D., Vallee, R. and Sodeik, B. (2002). Function of dynein and dynactin in herpes simplex virus capsid transport. *Mol Biol Cell* **13,** 2795-2809.

Esmann, J. (2001). The many challenges of facial herpes simplex virus infection. *J Antimicrob Chemother* **47 Suppl T1,** 17-27.

Fay, N. and Panté, N. (2015). Nuclear entry of DNA viruses. *Front Microbiol* **6,** 467.

Gianni, T., Amasio, M. and Campadelli-Fiume, G. (2009). Herpes simplex virus gD forms distinct complexes with fusion executors gB and gH/gL in part through the C-terminal profusion domain. *J Biol Chem* **284,** 17370-17382.

Gibson, W. and Roizman, B. (1972). Proteins specified by herpes simplex virus. 8. Characterization and composition of multiple capsid forms of subtypes 1 and 2. *J Virol* **10,** 1044-1052.

Goshima, F., Watanabe, D., Takakuwa, H., Wada, K., Daikoku, T., Yamada, M. and Nishiyama, Y. (2000). Herpes simplex virus UL17 protein is associated with B capsids and colocalizes with ICP35 and VP5 in infected cells. *Arch Virol* **145,** 417-426.

GREIFF, D., BLUMENTHAL, H., CHIGA, M. and PINKERTON, H. (1954). The effects on biological materials of freezing and drying by vacuum sublimation. II. Effect on influenza virus. *J Exp Med* **100,** 89-101.

Grunewald, K., Desai, P., Winkler, D.C., Heymann, J.B., Belnap, D.M., Baumeister, W. and Steven, A.C. (2003). Three-dimensional structure of herpes simplex virus from cryo-electron tomography. *Science* **302,** 1396-1398.

Hampar, B. and Copeland, M.L. (1965). Persistent Herpes Simplex Virus Infection In Vitro with Cycles of Cell Destruction and Regrowth. *J Bacteriol* **90,** 205-212.

Hansen, R.K., Zhai, S., Skepper, J.N., Johnston, M.D., Alpar, H.O. and Slater, N.K. (2005). Mechanisms of inactivation of HSV-2 during storage in frozen and lyophilized forms. *Biotechnol Prog* **21,** 911-917.

Heldwein, E.E. and Krummenacher, C. (2008). Entry of herpesviruses into mammalian cells. *Cellular and Molecular Life Sciences* **65,** 1653-1668.

Hicks, A.L. and Duffy, S. (2014). Cell tropism predicts long-term nucleotide substitution rates of mammalian RNA viruses. *PLoS Pathog* **10,** e1003838.

Honess, R.W. and Roizman, B. (1974). Regulation of herpesvirus macromolecular synthesis. I. Cascade regulation of the synthesis of three groups of viral proteins. *J Virol* **14,** 8-19.

Ikeda, K., Tsujimoto, K., Uozaki, M., Nishide, M., Suzuki, Y., Koyama, A.H. and Yamasaki, H. (2011). Inhibition of multiplication of herpes simplex virus by caffeic acid. *Int J Mol Med* **28,** 595-598.

Jackson, S.A. and DeLuca, N.A. (2003). Relationship of herpes simplex virus genome configuration to productive and persistent infections. *Proc Natl Acad Sci U S A* **100,** 7871-7876.

Jenkins, F.J. and Turner, S.L. (1996). Herpes simplex virus: a tool for neuroscientists. *Front Biosci* **1,** d241-247.

Johnson, D.C., Wisner, T.W. and Wright, C.C. (2011). Herpes simplex virus glycoproteins gB and gD function in a redundant fashion to promote secondary envelopment. *J Virol* **85,** 4910-4926.

Kang, M.H., Roy, B.B., Finnen, R.L., Le Sage, V., Johnston, S.M., Zhang, H. and Banfield, B.W. (2013). The Us2 gene product of herpes simplex virus 2 is a membrane-associated ubiquitin-interacting protein. *J Virol* **87,** 9590-9603.

Kolb, A.W., Larsen, I.V., Cuellar, J.A. and Brandt, C.R. (2015). Genomic, phylogenetic, and recombinational characterization of herpes simplex virus 2 strains. *J Virol* **89,** 6427-6434.

Kramer, M.F., Chen, S.H., Knipe, D.M. and Coen, D.M. (1998). Accumulation of viral transcripts and DNA during establishment of latency by herpes simplex virus. *J Virol* **72,** 1177-1185.

Kukhanova, M.K., Korovina, A.N. and Kochetkov, S.N. (2014). Human herpes simplex virus: life cycle and development of inhibitors. *Biochemistry (Mosc)* **79,** 1635-1652.

Lee, H.C. (2008) Comparative roles of herpes simplex virus type 1 (HSV-1) viral glycoproteins in cytoplasmic virion egress. In *Department of Pathobiological Sciences*. Louisiana, Louisiana State University.

Lehman, I.R. and Boehmer, P.E. (1999). Replication of herpes simplex virus DNA. *J Biol Chem* **274,** 28059-28062.

Looker, K.J., Garnett, G.P. and Schmid, G.P. (2008). An estimate of the global prevalence and incidence of herpes simplex virus type 2 infection. *Bull World Health Organ* **86,** 805-812, A.

Looker, K.J., Magaret, A.S., May, M.T., Turner, K.M., Vickerman, P., Gottlieb, S.L. and Newman, L.M. (2015a). Global and Regional Estimates of Prevalent and Incident Herpes Simplex Virus Type 1 Infections in 2012. *PLoS One* **10,** e0140765.

Looker, K.J., Magaret, A.S., Turner, K.M., Vickerman, P., Gottlieb, S.L. and Newman, L.M. (2015b). Correction: Global estimates of prevalent and incident herpes simplex virus type 2 infections in 2012. *PLoS One* **10,** e0128615.

Ma, J.Z., Russell, T.A., Spelman, T., Carbone, F.R. and Tscharke, D.C. (2014). Lytic gene expression is frequent in HSV-1 latent infection and correlates with the engagement of a cell-intrinsic transcriptional response. *PLoS Pathog* **10,** e1004237.

Martines, R.B., Ng, D.L., Greer, P.W., Rollin, P.E. and Zaki, S.R. (2015). Tissue and cellular tropism, pathology and pathogenesis of Ebola and Marburg viruses. *J Pathol* **235,** 153-174.

Martinez, V., Caumes, E. and Chosidow, O. (2008). Treatment to prevent recurrent genital herpes. *Curr Opin Infect Dis* **21,** 42-48.

Mayaud, P., Nagot, N., Konaté, I., Ouedraogo, A., Weiss, H.A., Foulongne, V.*, et al.* (2008). Effect of HIV-1 and antiretroviral therapy on herpes simplex virus type 2: a prospective study in African women. *Sex Transm Infect* **84,** 332-337.

Mettenleiter, T.C., Klupp, B.G. and Granzow, H. (2006). Herpesvirus assembly: a tale of two membranes. *Curr Opin Microbiol* **9,** 423-429.

Mettenleiter, T.C., Klupp, B.G. and Granzow, H. (2009). Herpesvirus assembly: an update. *Virus Res* **143,** 222-234.

Meyding-Lamadé, U. and Strank, C. (2012). Herpesvirus infections of the central nervous system in immunocompromised patients. *Ther Adv Neurol Disord* **5,** 279-296.

Mingo, R.M., Han, J., Newcomb, W.W. and Brown, J.C. (2012). Replication of herpes simplex virus: egress of progeny virus at specialized cell membrane sites. *J Virol* **86,** 7084-7097.

Nahmias, A.J. (1970). ANTIBODIES TO HERPESVIRUS-HOMINIS TYPES-1-AND-2 IN HUMANS .2. WOMEN WITH CERVICAL CANCER. *American Journal of Epidemiology* **91,** 547-&.

Newcomb, W.W., Homa, F.L. and Brown, J.C. (2006). Herpes simplex virus capsid structure: DNA packaging protein UL25 is located on the external surface of the capsid near the vertices. *J Virol* **80,** 6286-6294.

Newcomb, W.W., Trus, B.L., Cheng, N., Steven, A.C., Sheaffer, A.K., Tenney, D.J.*, et al.* (2000). Isolation of herpes simplex virus procapsids from cells infected with a protease-deficient mutant virus. *J Virol* **74,** 1663-1673.

Nguyen, M.L., Kraft, R.M. and Blaho, J.A. (2005). African green monkey kidney Vero cells require de novo protein synthesis for efficient herpes simplex virus 1-dependent apoptosis. *Virology* **336,** 274-290.

Nicola, A.V., McEvoy, A.M. and Straus, S.E. (2003). Roles for endocytosis and low pH in herpes simplex virus entry into HeLa and Chinese hamster ovary cells. *J Virol* **77,** 5324-5332.

Nicola, A.V. and Straus, S.E. (2004). Cellular and viral requirements for rapid endocytic entry of herpes simplex virus. *J Virol* **78,** 7508-7517.

Nicoll, M.P., Proença, J.T. and Efstathiou, S. (2012). The molecular basis of herpes simplex virus latency. *FEMS Microbiol Rev* **36,** 684-705.

Nozawa, C., Hattori, L.Y., Galhardi, L.C., Lopes, N., Bomfim, W.A., Cândido, L.K.*, et al.* (2014). Herpes simplex virus: isolation, cytopathological characterization and antiviral sensitivity. *An Bras Dermatol* **89,** 448-452.

Nunes, A., Borrego, M.J. and Gomes, J.P. (2013). Genomic features beyond Chlamydia trachomatis phenotypes: what do we think we know? *Infect Genet Evol* **16,** 392-400.

Owen, D.J., Crump, C.M. and Graham, S.C. (2015). Tegument Assembly and Secondary Envelopment of Alphaherpesviruses. *Viruses* **7,** 5084-5114.

Palmer, E.A. (2010) Studies on the herpes simplex virus type 1 UL32 DNA packaging protein. In *Faculty of Biomedical and Life Sciences*. Glasgow, University of Glasgow.

Pellet, P.E. and Roizman, B. (2003) *Herpesviridae*. In *Fields Virology*, D.M. Knipe, P.M. Howley (eds.) 6th Edition edn. Philadelphia, Lippinkott, Williams & Wilkins, pp. 1802-1822.

Perng, G.C. and Jones, C. (2010). Towards an understanding of the herpes simplex virus type 1 latency-reactivation cycle. *Interdiscip Perspect Infect Dis* **2010,** 262415.

Pinsky, N.A., Huddleston, J.M., Jacobson, R.M., Wollan, P.C. and Poland, G.A. (2003). Effect of multiple freeze-thaw cycles on detection of measles, mumps, and rubella virus antibodies. *Clin Diagn Lab Immunol* **10,** 19-21.

Ramachandran, S. (2003) Influence of herpes simplex virus type-1 glycoprotein B expression on viral pathogenecity and the $CD8^+$ T cell response. In *Faculty of School of Medicine*. Pittsburgh, University of Pittsburgh.

Reske, A., Pollara, G., Krummenacher, C., Chain, B.M. and Katz, D.R. (2007). Understanding HSV-1 entry glycoproteins. *Rev Med Virol* **17,** 205-215.

Roizman, B., Knipe, D.M. and Whitley, R. (2003) Herpes Simplex Viruses. In *Fields Virology*, D.M. Knipe, P.M. Howley (eds.) 6th Edition edn. Philadelphia, Lippinkott, Williams & Wilkins, pp. 1823-1897.

Rudnick, C.M. and Hoekzema, G.S. (2002). Neonatal herpes simplex virus infections. *American Family Physician* **65,** 1138-1142.

Salameh, S., Sheth, U. and Shukla, D. (2012). Early events in herpes simplex virus lifecycle with implications for an infection of lifetime. *Open Virol J* **6,** 1-6.

Schiffer, J.T. and Corey, L. (2013). Rapid host immune response and viral dynamics in herpes simplex virus-2 infection. *Nat Med* **19,** 280-290.

Sciubba, J.J. (2003). Herpes simplex and aphthous ulcerations: presentation, diagnosis and management--an update. *Gen Dent* **51,** 510-516.

Scrima, N., Lepault, J., Boulard, Y., Pasdeloup, D., Bressanelli, S. and Roche, S. (2015). Insights into herpesvirus tegument organization from structural analyses of the 970 central residues of HSV-1 UL36 protein. *J Biol Chem* **290,** 8820-8833.

Sheaffer, A.K., Newcomb, W.W., Gao, M., Yu, D., Weller, S.K., Brown, J.C. and Tenney, D.J. (2001). Herpes simplex virus DNA cleavage and packaging proteins associate with the procapsid prior to its maturation. *J Virol* **75,** 687-698.

Singh, A., Preiksaitis, J., Ferenczy, A. and Romanowski, B. (2005). The laboratory diagnosis of herpes simplex virus infections. *The Canadian journal of infectious diseases & medical microbiology = Journal canadien des maladies infectieuses et de la microbiologie medicale / AMMI Canada* **16,** 92-98.

Smith, J.S. and Robinson, N.J. (2002). Age-specific prevalence of infection with herpes simplex virus types 2 and 1: a global review. *J Infect Dis* **186 Suppl 1,** S3-28.

Spear, P.G. (2004). Herpes simplex virus: receptors and ligands for cell entry. *Cell Microbiol* **6,** 401-410.

Stevens, J.G. and Cook, M.L. (1971). LATENT HERPES SIMPLEX VIRUS IN SPINAL GANGLIA OF MICE. *Science* **173,** 843-&.

Straface, G., Selmin, A., Zanardo, V., De Santis, M., Ercoli, A. and Scambia, G. (2012). Herpes simplex virus infection in pregnancy. *Infect Dis Obstet Gynecol* **2012,** 385697.

Svec, D., Tichopad, A., Novosadova, V., Pfaffl, M.W. and Kubista, M. (2015). How good is a PCR efficiency estimate: Recommendations for precise and robust qPCR efficiency assessments. *Biomol Detect Quantif* **3,** 9-16.

Szpara, M.L., Gatherer, D., Ochoa, A., Greenbaum, B., Dolan, A., Bowden, R.J.*, et al.* (2014). Evolution and diversity in human herpes simplex virus genomes. *J Virol* **88,** 1209-1227.

Tada, A., Sekine, N., Toba, M. and Yoshino, K. (1977). An analysis of factors influencing the isolation rate of herpes simplex virus. *Microbiol Immunol* **21,** 219-229.

Tandon, R., Mocarski, E.S. and Conway, J.F. (2015). The A, B, Cs of herpesvirus capsids. *Viruses* **7,** 899-914.

Tang, Y.W., Mitchell, P.S., Espy, M.J., Smith, T.F. and Persing, D.H. (1999). Molecular diagnosis of herpes simplex virus infections in the central nervous system. *J Clin Microbiol* **37,** 2127-2136.

Trybala, E., Liljeqvist, J.A., Svennerholm, B. and Bergström, T. (2000). Herpes simplex virus types 1 and 2 differ in their interaction with heparan sulfate. *J Virol* **74,** 9106-9114.

Vahlne, A., Svennerholm, B., Sandberg, M., Hamberger, A. and Lycke, E. (1980). Differences in attachment between herpes simplex type 1 and type 2 viruses to neurons and glial cells. *Infect Immun* **28,** 675-680.

Wagner, E.K. and Bloom, D.C. (1997). Experimental investigation of herpes simplex virus latency. *Clin Microbiol Rev* **10,** 419-443.

Weller, S.K. and Coen, D.M. (2012). Herpes simplex viruses: mechanisms of DNA replication. *Cold Spring Harb Perspect Biol* **4,** a013011.

Whitley, R.J., Kimberlin, D.W. and Roizman, B. (1998). Herpes simplex viruses. *Clin Infect Dis* **26,** 541-553; quiz 554-545.

Whitley, R.J. and Roizman, B. (2001). Herpes simplex virus infections. *Lancet* **357,** 1513-1518.

Zhou, Z.H., He, J., Jakana, J., Tatman, J.D., Rixon, F.J. and Chiu, W. (1995). Assembly of VP26 in herpes simplex virus-1 inferred from structures of wild-type and recombinant capsids. *Nat Struct Biol* **2,** 1026-1030.

Appendices

Appendix 1 – Standard and amplification curves

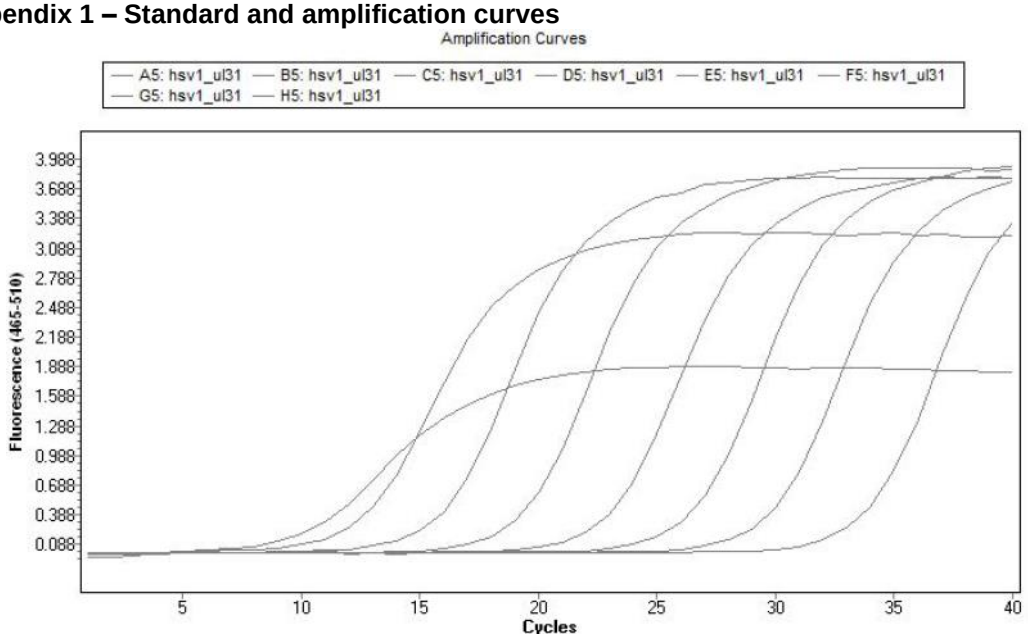

Figure A.1: UL31 amplification curves.

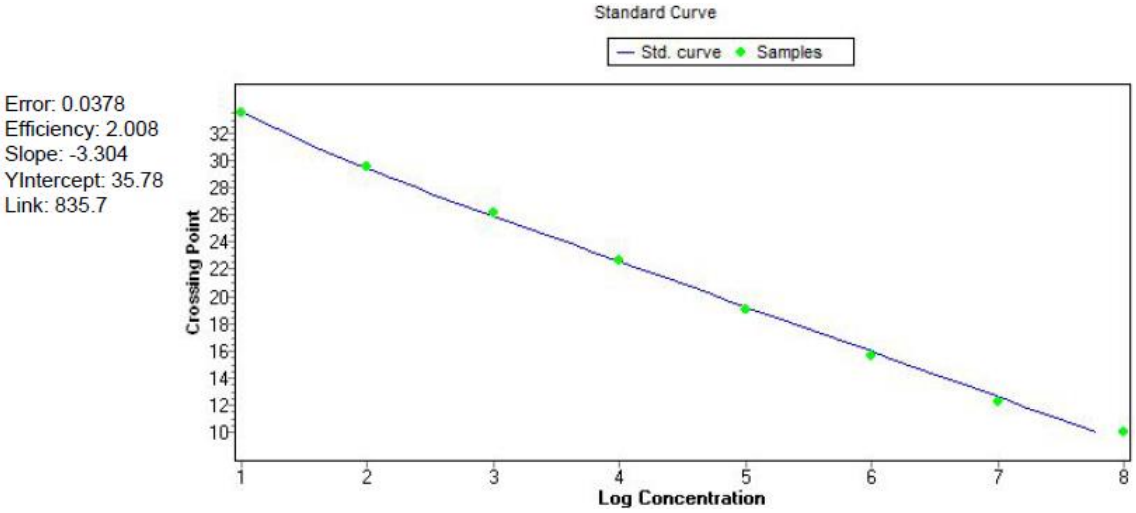

Figure A.2: UL31 standard curve.

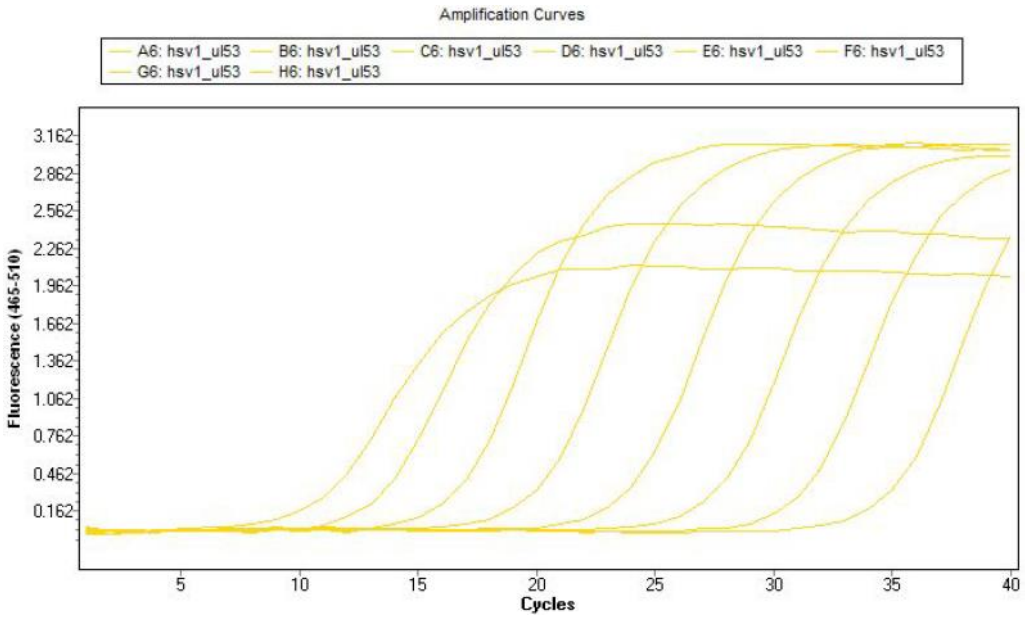

Figure A.3: UL53 amplification curves.

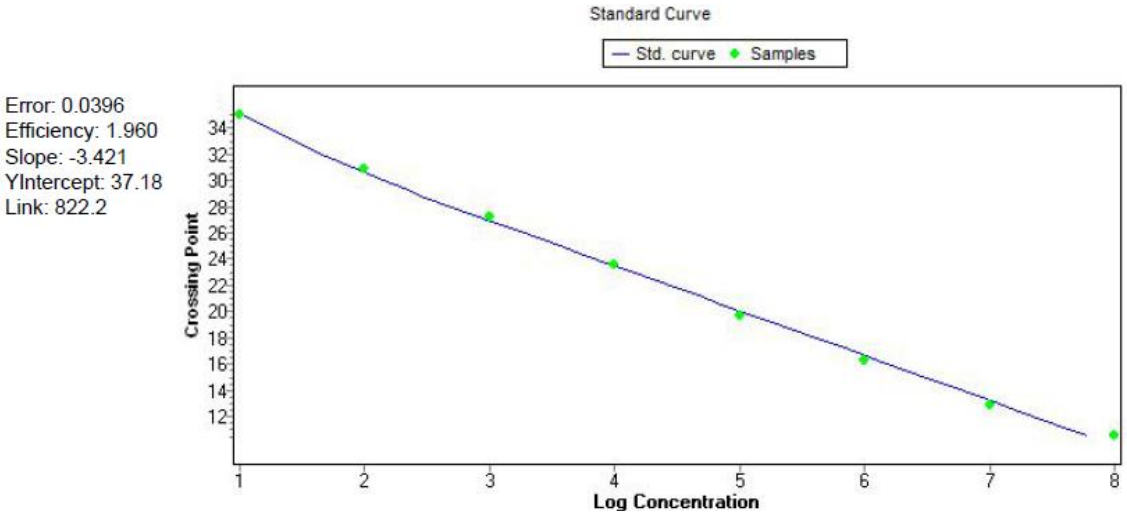

Figure A.4: UL53 standard curve.

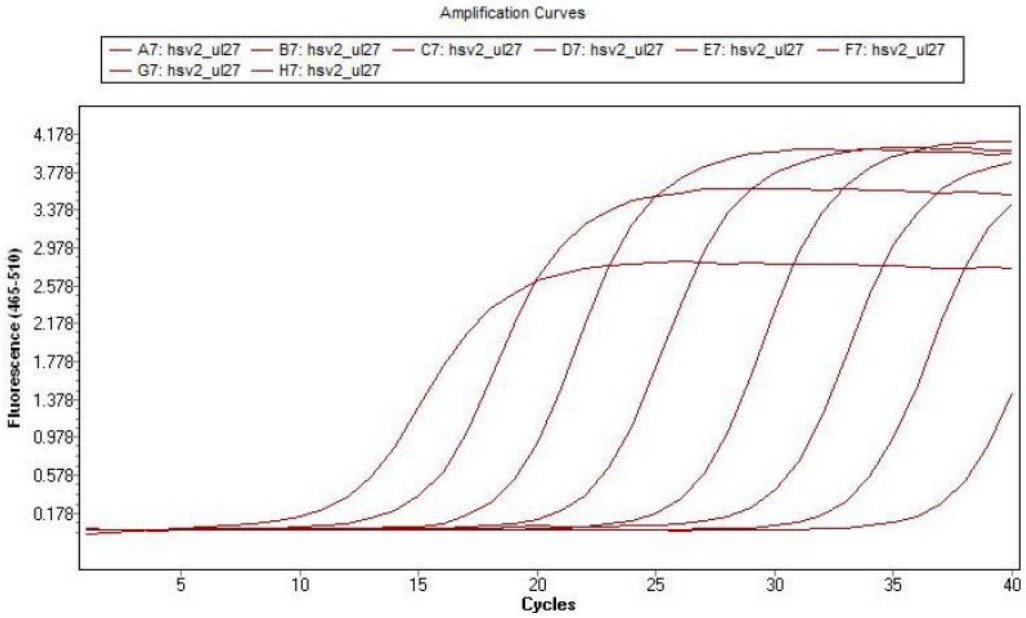

Figure A.5: UL27 amplification curves.

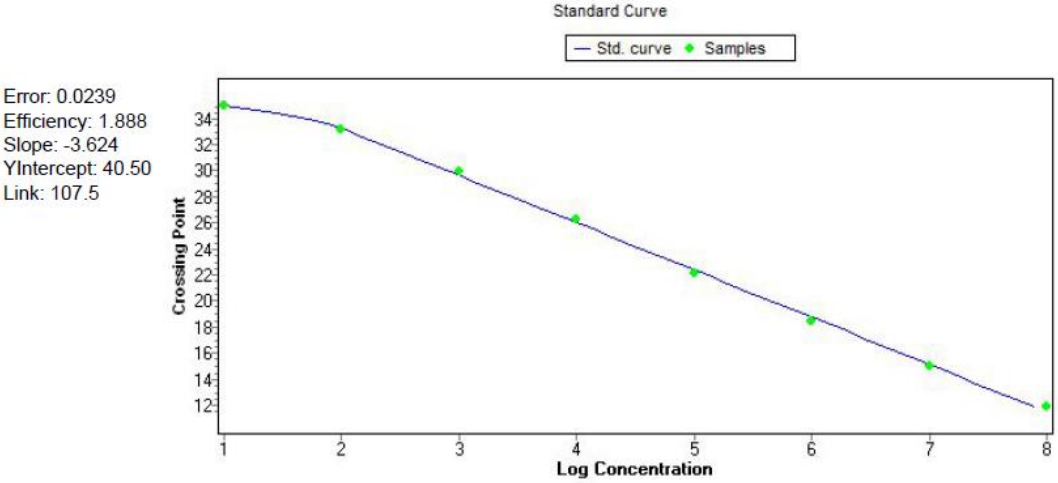

Figure A.6: UL27 standard curve.

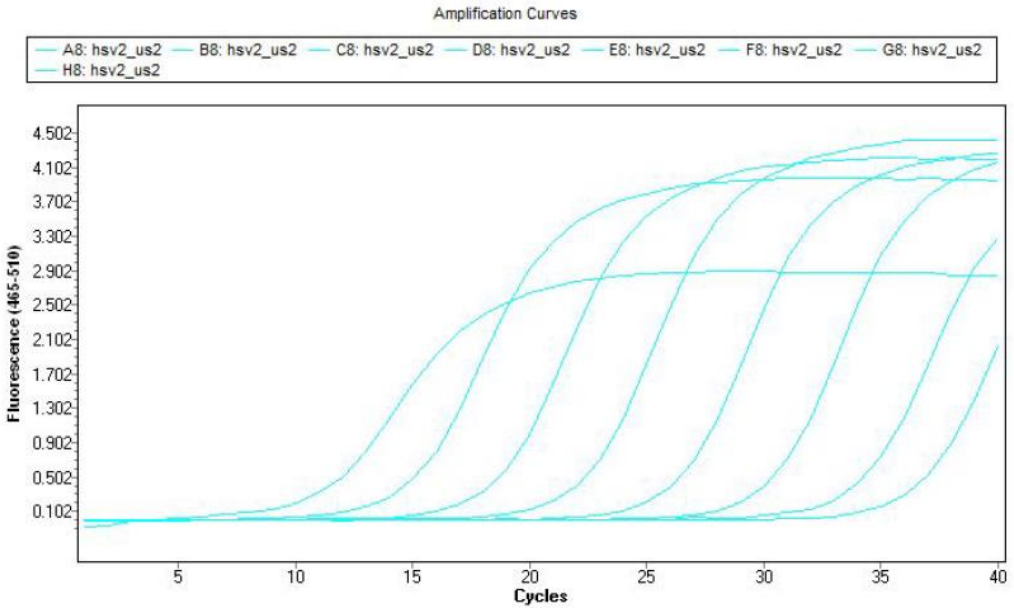

Figure A.7: US2 amplification curves.

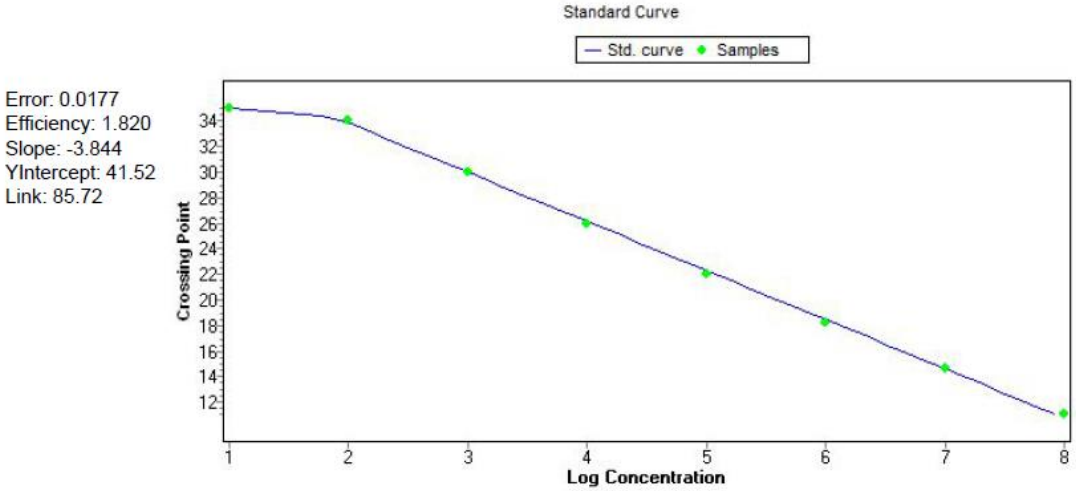

Figure A.8: US2 standard curve.

Appendix 2 – Preliminary assays kPCR results

Table A.1: Preliminary assays qPCR results, for each time-point, and both inoculation processes tested.

Process	Time-points	Centrifugation	Agitation
Sample 1	**4h**	$8{,}61 \times 10^{6}$	$1{,}92 \times 10^{7}$
	7h	$1{,}08 \times 10^{7}$	$1{,}88 \times 10^{7}$
	9h	$3{,}66 \times 10^{7}$	$1{,}35 \times 10^{7}$
	13h	$1{,}16 \times 10^{8}$	$2{,}70 \times 10^{7}$
	18h	$1{,}86 \times 10^{8}$	$5{,}36 \times 10^{7}$
	23h	$2{,}80 \times 10^{8}$	$1{,}05 \times 10^{8}$
	29h	$2{,}62 \times 10^{8}$	$9{,}65 \times 10^{7}$
Sample 2	**4h**	$2{,}75 \times 10^{7}$	$6{,}57 \times 10^{7}$
	7h	$4{,}03 \times 10^{7}$	$4{,}14 \times 10^{7}$
	9h	$7{,}60 \times 10^{7}$	$7{,}26 \times 10^{7}$
	13h	$1{,}55 \times 10^{8}$	$1{,}22 \times 10^{8}$
	18h	$2{,}32 \times 10^{8}$	$1{,}66 \times 10^{8}$
	23h	$4{,}32 \times 10^{8}$	$2{,}87 \times 10^{8}$
	29h	$2{,}79 \times 10^{8}$	$2{,}62 \times 10^{8}$

Appendix 3 – qPCR results

Table A.2: Sample A qPCR results for each time-point, in three cell lines and four different MOIs

Virus Sample	Cell Line	Time points	MOI 0.1	MOI 1	MOI 10	MOI 100
HSV-1 Sample A	HeLa 229	0h	$1{,}10 \times 10^{5}$	$7{,}34 \times 10^{6}$	$1{,}55 \times 10^{8}$	$1{,}69 \times 10^{9}$
		6h	$8{,}32 \times 10^{4}$	$3{,}59 \times 10^{6}$	$6{,}22 \times 10^{7}$	$6{,}82 \times 10^{8}$
		12h	$9{,}28 \times 10^{4}$	$1{,}00 \times 10^{7}$	$9{,}78 \times 10^{7}$	$1{,}32 \times 10^{9}$
		18h	$1{,}68 \times 10^{6}$	$3{,}59 \times 10^{7}$	$3{,}54 \times 10^{8}$	$3{,}23 \times 10^{9}$
		24h	$1{,}41 \times 10^{7}$	$1{,}21 \times 10^{8}$	$1{,}59 \times 10^{9}$	$1{,}19 \times 10^{10}$
		30h	$3{,}04 \times 10^{7}$	$4{,}05 \times 10^{8}$	$3{,}3 \times 10^{9}$	$3{,}10 \times 10^{10}$
	Vero	0h	$1{,}90 \times 10^{6}$	$1{,}48 \times 10^{7}$	$1{,}47 \times 10^{8}$	$7{,}55E \times 10^{8}$
		6h	$1{,}01 \times 10^{6}$	$7{,}36 \times 10^{6}$	$9{,}58 \times 10^{7}$	$1{,}20 \times 10^{9}$
		12h	$3{,}15 \times 10^{6}$	$4{,}14 \times 10^{6}$	$8{,}54 \times 10^{7}$	$1{,}08 \times 10^{9}$
		18h	$8{,}60 \times 10^{5}$	$1{,}09 \times 10^{7}$	$1{,}38 \times 10^{8}$	$1{,}35 \times 10^{9}$
		24h	$5{,}12 \times 10^{6}$	$2{,}47 \times 10^{7}$	$2{,}99 \times 10^{8}$	$2{,}02 \times 10^{9}$
		30h	$7{,}22 \times 10^{6}$	$5{,}80 \times 10^{7}$	$7{,}04 \times 10^{8}$	$7{,}42 \times 10^{9}$
	Vero E6	0h	$7{,}22 \times 10^{5}$	$1{,}86 \times 10^{6}$	$3{,}37 \times 10^{7}$	$3{,}76 \times 10^{8}$
		6h	$3{,}65 \times 10^{5}$	$1{,}10 \times 10^{6}$	$7{,}62 \times 10^{6}$	$6{,}62 \times 10^{7}$
		12h	$1{,}63 \times 10^{5}$	$1{,}70 \times 10^{6}$	$1{,}71 \times 10^{7}$	$1{,}45 \times 10^{8}$
		18h	$1{,}15 \times 10^{6}$	$6{,}28 \times 10^{6}$	$6{,}48 \times 10^{7}$	$8{,}08 \times 10^{8}$
		24h	$2{,}53 \times 10^{6}$	$2{,}91 \times 10^{7}$	$2{,}82 \times 10^{8}$	$2{,}22 \times 10^{9}$
		30h	$4{,}39 \times 10^{6}$	$7{,}10 \times 10^{7}$	$6{,}18 \times 10^{8}$	$3{,}94 \times 10^{9}$

Table A.3: Sample B qPCR results for each time-point, in three cell lines and four different MOIs

Virus Sample	Cell Line	Time points	MOI 0.1	MOI 1	MOI 10	MOI 100
HSV-1 Sample B	HeLa 229	0h	$1{,}40 \times 10^{5}$	$2{,}29 \times 10^{7}$	$1{,}85 \times 10^{8}$	$1{,}23 \times 10^{9}$
		6h	$2{,}41 \times 10^{5}$	$3{,}59 \times 10^{6}$	$3{,}94 \times 10^{7}$	$6{,}22 \times 10^{8}$
		12h	$3{,}91 \times 10^{5}$	$4{,}99 \times 10^{6}$	$4{,}96 \times 10^{7}$	$4{,}82 \times 10^{8}$
		18h	$3{,}05 \times 10^{6}$	$1{,}56 \times 10^{7}$	$1{,}61 \times 10^{8}$	$1{,}49 \times 10^{9}$
		24h	$6{,}68 \times 10^{6}$	$4{,}30 \times 10^{7}$	$4{,}70 \times 10^{8}$	$4{,}70 \times 10^{9}$
		30h	$3{,}08 \times 10^{7}$	$1{,}39 \times 10^{8}$	$1{,}25 \times 10^{9}$	$9{,}40 \times 10^{9}$
	Vero	0h	$2{,}81 \times 10^{6}$	$4{,}01 \times 10^{7}$	$3{,}11 \times 10^{8}$	$2{,}17 \times 10^{9}$
		6h	$3{,}46 \times 10^{6}$	$2{,}37 \times 10^{7}$	$2{,}08 \times 10^{8}$	$3{,}30 \times 10^{9}$
		12h	$1{,}37 \times 10^{6}$	$2{,}30 \times 10^{7}$	$1{,}99 \times 10^{8}$	$2{,}57 \times 10^{9}$
		18h	$9{,}16 \times 10^{6}$	$5{,}30 \times 10^{7}$	$5{,}04 \times 10^{8}$	$5{,}03 \times 10^{9}$
		24h	$1{,}44 \times 10^{7}$	$1{,}30 \times 10^{8}$	$1{,}45 \times 10^{9}$	$9{,}78 \times 10^{9}$
		30h	$3{,}07 \times 10^{7}$	$2{,}85 \times 10^{8}$	$3{,}12 \times 10^{9}$	$2{,}00 \times 10^{10}$
	Vero E6	0h	$8{,}08 \times 10^{5}$	$3{,}29 \times 10^{6}$	$3{,}29 \times 10^{7}$	$4{,}68 \times 10^{8}$
		6h	$6{,}14 \times 10^{5}$	$1{,}73 \times 10^{6}$	$1{,}10 \times 10^{7}$	$1{,}49 \times 10^{8}$
		12h	$8{,}78 \times 10^{5}$	$4{,}75 \times 10^{6}$	$3{,}54 \times 10^{7}$	$4{,}08 \times 10^{8}$
		18h	$1{,}97 \times 10^{6}$	$2{,}25 \times 10^{7}$	$1{,}38 \times 10^{8}$	$1{,}63 \times 10^{9}$
		24h	$6{,}80 \times 10^{6}$	$7{,}26 \times 10^{7}$	$7{,}40 \times 10^{8}$	$5{,}26 \times 10^{9}$
		30h	$1{,}45 \times 10^{7}$	$1{,}93 \times 10^{8}$	$1{,}40 \times 10^{9}$	$8{,}20 \times 10^{9}$

Table A.4: Sample C qPCR results for each time-point, in three cell lines and four different MOIs

Virus Sample	Cell Line	Time points	MOI 0.1	MOI 1	MOI 10	MOI 100
HSV-2 Sample C	HeLa 229	0h	$3{,}06 \times 10^4$*	$8{,}68 \times 10^4$	$1{,}17 \times 10^6$	$8{,}96 \times 10^6$
		6h	$3{,}06 \times 10^4$	$1{,}72 \times 10^4$	$1{,}02 \times 10^6$	$8{,}44E \times 10^6$
		12h	**	$1{,}23 \times 10^5$	$1{,}16 \times 10^6$	$8{,}92 \times 10^6$
		18h	$3{,}39 \times 10^4$*	$6{,}22 \times 10^5$	$2{,}58 \times 10^6$	$3{,}96 \times 10^7$
		24h	$2{,}14 \times 10^5$	$2{,}80 \times 10^6$	$1{,}32 \times 10^7$	$1{,}39 \times 10^8$
		30h	$2{,}62 \times 10^5$	$3{,}50 \times 10^6$	$3{,}47 \times 10^7$	$2{,}33 \times 10^8$
	Vero	0h	$5{,}70 \times 10^3$	$1{,}83 \times 10^5$	$1{,}70 \times 10^6$	$1{,}37 \times 10^7$
		6h	$1{,}88 \times 10^4$	$7{,}21 \times 10^4$	$7{,}66 \times 10^5$	$1{,}58 \times 10^7$
		12h	$1{,}07 \times 10^4$	$8{,}40 \times 10^4$	$5{,}12 \times 10^5$	$8{,}74 \times 10^6$
		18h	$1{,}22 \times 10^4$	$2{,}86 \times 10^5$	$1{,}72 \times 10^6$	$1{,}95 \times 10^7$
		24h	$6{,}66E \times 10^3$	$9{,}20 \times 10^5$	$8{,}62 \times 10^6$	$5{,}44 \times 10^7$
		30h	$1{,}48 \times 10^5$	$1{,}75 \times 10^6$	$1{,}47 \times 10^7$	$1{,}18 \times 10^8$
	Vero E6	0h	$1{,}63 \times 10^3$*	$8{,}48 \times 10^3$	$5{,}42 \times 10^4$	$1{,}00 \times 10^6$
		6h	**	$2{,}39 \times 10^3$	$5{,}30 \times 10^4$	$5{,}98 \times 10^5$
		12h	$1{,}63 \times 10^3$	$9{,}08 \times 10^3$	$1{,}85 \times 10^5$	$3{,}89 \times 10^6$
		18h	$2{,}42 \times 10^4$	$2{,}07 \times 10^5$	$2{,}10 \times 10^6$	$2{,}12 \times 10^7$
		24h	$6{,}36 \times 10^4$	$6{,}46 \times 10^5$	$1{,}54 \times 10^7$	$1{,}12 \times 10^8$
		30h	$1{,}59 \times 10^5$	$1{,}90 \times 10^6$	$3{,}39 \times 10^7$	$1{,}44 \times 10^8$

* For growth curve generation, to these points was given the viral load quantified in the next time-point;

** Results were inconclusive